

CAUSAL ORDER: THE KEY TO LEVERAGING IMPERFECT EXPERTS IN CAUSAL INFERENCE

Anonymous authors

Paper under double-blind review

ABSTRACT

Large Language Models (LLMs) have recently been used as *experts* to infer causal graphs, often by repeatedly applying a pairwise prompt that asks about the causal relationship of each variable pair. However, such experts, including human domain experts, cannot distinguish between direct and indirect effects given a pairwise prompt. Therefore, instead of the graph, we propose that *causal order* be used as a more stable output interface for utilizing expert knowledge. When querying a *perfect* expert with a pairwise prompt, we show that the inferred graph can have significant errors whereas the causal order is always correct. In practice, however, LLMs are imperfect experts and we find that pairwise prompts lead to multiple cycles and do not yield a valid order. Hence, we propose a prompting strategy that introduces an auxiliary variable for every variable pair and instructs the LLM to avoid cycles within this triplet. We show, both theoretically and empirically, that such a *triplet* prompt leads to fewer cycles than the pairwise prompt. Across multiple real-world graphs, the triplet prompt yields a more accurate order using both LLMs and human annotators as experts. By querying the expert with different auxiliary variables for the same variable pair, it also increases robustness—triplet method with much smaller models such as Phi-3 and Llama-3 8B outperforms a pairwise prompt with GPT-4. For practical usage, we show how the estimated causal order from the triplet method can be used to reduce error in downstream discovery and effect inference tasks.

1 INTRODUCTION

Based on evidence that LLMs’ domain knowledge, even if imperfect, can be used to decide the direction of causal relationship between a pair of variables (Kıcıman et al., 2023; Willig et al., 2022), recent years have seen the use of LLMs for inferring the entire causal graph for a given problem domain. This is done by typically invoking a pairwise prompt—of the form: “does variable *A* cause variable *B*?”—multiple times for different pairs of variables (Long et al., 2022; Antonucci et al., 2023; Kıcıman et al., 2023; Cohrs et al., 2023). In other related efforts, causal graphs or edges obtained from LLMs are used as a prior (Takayama et al., 2024) or constraint (Long et al., 2023; Khatibi et al., 2024; Ban et al., 2023a) for causal discovery algorithms, showing that such graphs obtained from LLMs can improve downstream accuracy of graph discovery.

In this work, we however observe a key limitation of using graphs as the *output interface* for such domain knowledge inferred from LLMs, or for that matter, even other imperfect experts (e.g. humans). Obtaining the complete graph requires distinguishing between direct and indirect effects among variables. Given only a pair of variables, it is not possible to decide whether an edge exists or it is mediated by another variable, even for a perfect human expert – the existence of an edge depends on which other variables are considered to be a part of the node set in the query. For e.g., consider the true data-generating process, *Smoking* \rightarrow *Lung Damage* \rightarrow *Respiratory Diseases*. If an expert is asked whether there should be a direct causal edge from *Smoking* to *Respiratory Diseases*, they would answer “Yes”, which may not capture the true process. However, if they are told that the set of observed variables additionally includes *Lung Damage*, then the correct answer would be to not create a direct edge between *Smoking* and *Respiratory Diseases*, but rather create edges mediated through *Lung Damage*. In large graphs, keeping track of the different variables that can affect a given pairwise decision can be cumbersome.

As another example showing the subjectivity of deciding direct or indirect edges, consider the scenario in Fig 1 with the variables: *Pollution Exposure*, *Cancer*, *Dyspnoea*, *Smoking History* and *positive X-ray*. When queried only for the presence of a causal edge from *Pollution* to *Dyspnoea* (shortness of breath), an expert may answer “Yes”. However, if one has to provide a complete graph, it may be non-trivial for an expert to decisively agree on adding a direct edge from *Pollution* to *Dyspnoea*, creating edges mediating through *Cancer*, or both.

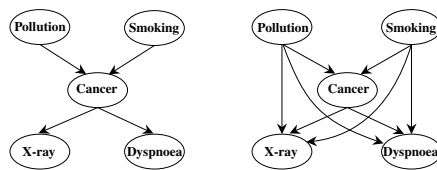


Figure 1: **Cancer dataset** (Scutari & Denis, 2014): *Left*: True causal graph. *Right*: Expert-estimated causal graph. Note that the latter, while not correct wrt. the true graph, yields the correct causal order. We leverage this observation in this work.

Causal Order: Significance and Utility. We instead propose *causal order* as an alternate but more stable approach to obtain experts’ domain knowledge, which can thereby improve downstream causal algorithms.

Causal order is defined as the topological ordering over graph variables. Since the causal order does not distinguish between direct and indirect effects, in both examples above, the causal order is unique and unambiguous. In the first example, $Smoking \prec Respiratory\ Diseases$ is a valid causal order ($a \prec b$ indicates that a occurs before b in a casual process). Similarly, in the second example, the causal order, $Pollution \prec Dyspnoea$ holds true in all three cases that the expert considered above. Formally, we show that for an (optimal) perfect expert that is given only a pair of variables at a time, the predicted causal graph can be incorrect but the predicted causal order is always correct. As a result, the standard practice of obtaining a causal graph from LLMs and crowd-sourced human annotators (using pairwise questions) may include many errors in the inferred edges, leading to further errors in the downstream causal algorithms; which can be alleviated using a causal order. Moreover, order is a more stable causal construct since it does not depend on the existence of other variables in the query, thus being more generalizable to new scenarios or datasets.

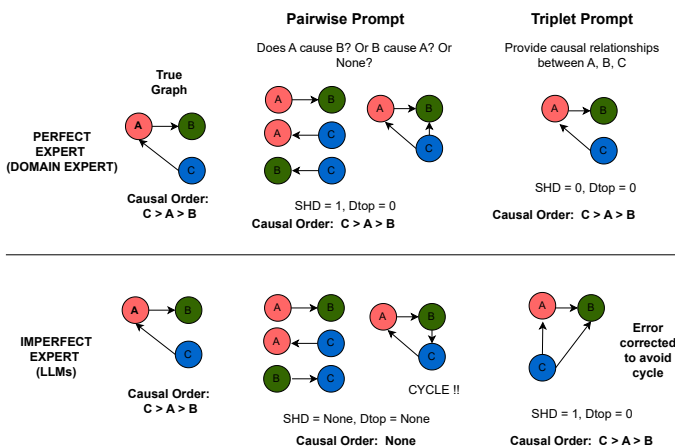


Figure 2: **Top**: Using the pairwise prompt, even under a perfect expert (domain expert), the estimated graph may not be correct ($SHD = 1$). Causal order, however, is correct ($D_{top} = 0$) and hence a better metric. **Bottom**: under imperfect experts (like LLMs), pairwise prompts may not lead to valid order, creating cycles. The proposed triplet prompting strategy alleviates this issue to provide better estimates of causal order ($D_{top} = 0$).

Although the causal order is a simpler structure than the full graph, it is useful by itself, aiding downstream tasks like effect inference and graph discovery. We show that the correct causal order is sufficient for identifying a valid backdoor set for any pair of treatment and outcome variables. Moreover, a causal order-based metric, topological divergence (D_{top}), correlates better with the effect estimation accuracy than commonly used graph metrics such as structural hamming distance (SHD). Specifically, $D_{top} = 0$ if and only if the causal order provides a valid backdoor adjustment set. In addition to effect inference, causal order can also be used to improve the accuracy of graph discovery algorithms. To this end, we provide simple algorithms for using causal order to improve existing causal discovery algorithms.

Causal Order: Eliciting from Experts. In practice, obtaining causal order from experts is still a challenge because we need to account for *imperfect experts* such as crowdsourced human annotators and LLMs. Using the standard method (Kiciman et al., 2023; Long et al., 2022) of iterating with a pairwise prompt/question over a set of variables, while a perfect expert would always predict the correct causal order, we find that using LLMs as experts leads to many cycles. To reduce the number

of cycles from LLM output, we propose a novel *triplet-based* prompting strategy for obtaining causal order. Rather than asking questions about a pair of variables, the triplet prompt asks about the causal relationship between the pair and an auxiliary variable, and instructs the LLM to obey acyclicity. We theoretically show that given an imperfect expert with an error ϵ on each prediction, using the triplet-based prompt results in an error less than ϵ , which is less than the error of the pairwise prompt. Moreover, since each variable pair occurs in more than one triplet, the redundancy allows for ensembling strategies for a more reliable order. Using both human annotators and LLMs as imperfect experts, we find that our triplet method provides more accurate causal order than the pairwise prompt, an observation that is accentuated in large graphs. The proposed triplet strategy provides accurate output even with small language models such as Phi-3 and Llama-3 8B to outperform the accuracy of pairwise prompts using GPT-4.

Our key contributions, validated using comprehensive experiments using both LLMs and human annotators as imperfect experts, can be summarized as: (1) suitability of causal order as the output interface of experts’ domain knowledge (studied both theoretically and empirically); (2) a new triplet prompting strategy in eliciting causal order from experts (especially relevant for imperfect experts); and (3) improved performance in downstream tasks using the causal order on both causal discovery and effect inference.

2 RELATED WORK

Domain Expertise-aided Causal Discovery. Prior knowledge has been used in causal discovery literature (Hasan & Gani, 2022; Constantinou et al., 2023; Heckerman & Geiger, 2013; Teshima & Sugiyama, 2021; O’Donnell et al., 2006; Wallace et al., 1996). These methods rely on prior knowledge such as domain expert opinions and documented knowledge from randomized controlled trials (RCT). Various priors have been studied in literature, such as *edge existence*, *forbidden edge* (Meek, 1995), *ancestral constraints* (Constantinou et al., 2023; Ban et al., 2023b). Recent advancements in LLMs have led to more attention on how LLMs may act as imperfect experts and provide causal knowledge based on metadata such as variable names (Kiciman et al., 2023; Ban et al., 2023b; Long et al., 2023; Willig et al., 2022). Early methods (Kiciman et al., 2023; Willig et al., 2022; Long et al., 2022) rely on LLMs to predict the complete causal structure, which is evaluated using metrics for full graph structure such as Structural Hamming Distance (SHD). Recent methods however use LLM’s output to improve accuracy of graph discovery algorithms. The key idea is that LLM can provide information about edges in the graph, which can then be added as a prior or constraint (Long et al., 2023; Jiralerspong et al., 2024) to reduce the search space for a causal discovery algorithm. For example, (Long et al., 2023) use LLMs to improve output of a constraint-based algorithm for full graph discovery by orienting undirected edges in the CPDAG. Most of these works, however, depend on obtaining correct edge information from LLMs and evaluate LLMs’ quality by full graph metrics (Naik et al., 2023; Zhang et al., 2024) such as SHD (Kiciman et al., 2023; Long et al., 2023). We observe that imperfect experts (LLMs or humans) cannot reliably provide edge information given a pair (or subset) of variables. Causal order may be a more appropriate causal structure to elicit from experts. For the same reason, the quality of an imperfect expert’s output for such tasks is better evaluated on the accuracy of causal order, rather than the full graph structure.

LLM-based Prompting Strategies. Existing LLM-based algorithms for graph discovery (Kiciman et al., 2023; Long et al., 2022; Ban et al., 2023b; Antonucci et al., 2023) use a pairwise prompt, essentially asking “does A cause B?” with varying levels of prompt complexity. Going beyond this line of work, we propose a triplet-based prompt that provides more accurate answers through aggregation and provides an uncertainty score for each edge to aid in cycle removal. As a result, our triplet-based prompt may be of independent interest for causal tasks.

3 CAUSAL ORDER: A STABLE INTERFACE FOR EXPERTS’ KNOWLEDGE

Preliminaries. Let $\mathcal{G}(\mathbf{X}, \mathbf{E})$ be a causal directed acyclic graph (DAG) consisting of a set of variables $\mathbf{X} = \{X_1, \dots, X_n\}$ and a set of directed edges \mathbf{E} among variables in \mathbf{X} . A directed edge $X_i \rightarrow X_j \in \mathbf{E}$ denotes the *direct* causal influence of X_i on X_j . Let $pa(X_i) = \{X_k | X_k \rightarrow X_i\}$, $de(X_i) = \{X_k | X_k \leftarrow \dots \leftarrow X_i\}$, $ch(X_i) = \{X_k | X_i \rightarrow X_k\}$ denote the set of *parents*, *descendants* and *children* of X_i respectively. If a variable X_k is a descendant of X_i (but they are not connected by a direct edge), then X_i is said to have an indirect effect on X_k . Average causal effect (Pearl, 2009) (ACE) of a variable X_i on a variable X_j is defined as: $ACE_{X_i}^{X_j} = \mathbb{E}[X_j | do(X_i = x_i)] - \mathbb{E}[X_j | do(X_i = x_i^*)]$, where X_i is called the *treatment*, X_j

is called the *target*, and $do(X_i = x_i)$ denotes an external intervention to the variable X_i with the value x_i . If a set of variables \mathbf{Z} satisfies the backdoor criterion (Defn. B.1) relative to (X_i, X_j) , $\mathbb{E}[X_j|do(X_i = x_i)]$ can be computed as: $\mathbb{E}[X_j|do(X_i = x_i)] = \mathbb{E}_{\mathbf{z} \sim \mathbf{Z}} \mathbb{E}[X_j|X_i = x_i, \mathbf{Z} = \mathbf{z}]$ (Thm. 3.3.2 of (Pearl, 2009)); and \mathbf{Z} is called a valid *adjustment set*. We now define the causal (topological) order and the topological divergence metric (Rolland et al., 2022) that measures the goodness of a given causal order wrt. the ground-truth graph.

Definition 3.1. Topological Order. Given a causal graph $\mathcal{G}(\mathbf{X}, \mathbf{E})$, a sequence (or ordered permutation) π of variables \mathbf{X} is a topological order iff for each edge $X_i \rightarrow X_j \in \mathbf{E}$, $\pi_i < \pi_j$.

Definition 3.2. Topological Divergence (Rolland et al., 2022). The topological divergence of an estimated order $\hat{\pi}$ with ground truth adjacency matrix A , denoted by $D_{top}(\hat{\pi}, A)$, is defined as:

$$D_{top}(\hat{\pi}, A) = \sum_{i=1}^n \sum_{j:\pi_i > \hat{\pi}_j} A_{ij} \quad (1)$$

where $A_{ij} = 1$ if there is a directed edge from node i to j else $A_{ij} = 0$. $D_{top}(\hat{\pi}, A)$ counts the number of ground-truth edges that cannot be recovered due to the estimated topological order $\hat{\pi}$.

Structural Hamming Distance (SHD) is also a popular metric for assessing the goodness of a predicted DAG. Given a true DAG \mathcal{G} and an estimated DAG $\hat{\mathcal{G}}$, SHD counts the number of missing, falsely detected, and falsely directed edges in $\hat{\mathcal{G}}$. D_{top} acts as a lower-bound on SHD (Rolland et al., 2022).

3.1 CAUSAL ORDER FROM A PERFECT EXPERT IS ALWAYS ACCURATE, BUT GRAPH IS NOT

The predominant existing approach to extract causal knowledge from LLMs is to use a pairwise prompt (Kiciman et al., 2023; Long et al., 2022; Choi et al., 2022) to determine the existence of an edge and then aggregate to build a causal graph. We herein detail a key limitation of using pairwise prompts to obtain the causal graph, even when using a hypothetical perfect expert (LLMs do make mistakes and are thus *imperfect* experts).

Revisiting the two graphs in Fig 1, the second graph is estimated by asking pairwise questions to a (perfect) expert that (hypothetically) knows about all cause-effect relationships in a domain (see Defn. 3.3 for a formal definition). The difference in edge predictions is introduced due to the existence of direct and indirect effects. For example, when asked about the relationship between *Pollution* and *Dyspnoea*, it may be valid to draw a direct edge if the expert is not aware of the *Cancer* node. As a result, if we compare the estimated graph in Fig 1 using standard graph comparison metrics such as SHD, we may find that that the estimated graph is significantly different from the true graph and (incorrectly) conclude that the expert’s knowledge was insufficient. Instead, if we compute the causal order using Def. 3.1 for the predicted graph (Fig 1 right), we obtain $\{Smoking, Pollution\} \prec Cancer \prec \{Dyspnoea, X-ray\}$. This order is fully consistent with the true graph (Fig 1 left), and thus is a valid causal order. We could thus correctly validate the expert’s knowledge as perfect. In particular, using causal order as the *output interface* of the expert-estimated graph ensures that no incorrect constraints are added. If the expert was asked to output the entire graph, erroneous edge constraints such as $Pollution \rightarrow Dyspnoea$ may be added to a downstream discovery algorithm. However, causal order only constrains that some path exists from *Pollution* to *Dyspnoea*, and allows the downstream algorithm to learn the correct edges from data.

As stated earlier, given a pair of variables, it is not possible to determine whether an edge exists between them, without knowing whether potential mediators between the two variables exist. By not explicitly storing edges, causal order instead corresponds to an ancestor-descendant relationship between a pair of variables which can be objectively decided given only the two variables. One can view our approach to causal order as formalizing the intuition in (Ban et al., 2023b) who consider an LLM’s pairwise answer to represent ancestor relationship between a pair of variables. We now formally show that causal order is a more accurate measure of an expert’s knowledge. All proofs are provided in Appendix B.

Definition 3.3. Perfect Expert. A perfect expert is an entity with access to the full ground-truth DAG $\mathcal{G}(\mathbf{X}, \mathbf{E})$. Given two variables two variables, $X_i, X_j \in \mathbf{X}$, and (optionally) an auxiliary set of nodes $\mathbf{O}_{ij} \subset \mathbf{X}$ (note that rest of the variables in set $\mathbf{U} = \mathbf{X} \setminus \mathbf{O}_{ij} \cup \{X_i, X_j\}$ need not be known), the expert can provide information on the existence of a causal edge between X_i and X_j (“does X_i cause X_j ”) as follows:

- $X_i \rightarrow X_j$: If there is directed edge from X_i to X_j ($X_i \rightarrow X_j \in \mathbf{E}$), or if a directed path exists from X_i to X_j such that it does not contain any node $Z \in \mathbf{O}_{ij}$.

- $X_j \rightarrow X_i$: If there is directed edge from X_j to X_i ($X_j \rightarrow X_i \in \mathbf{E}$), or if a directed path exists from X_j to X_i such that it does not contain any node $Z \in \mathbf{O}_{ij}$.
- Otherwise, output no edge.

Definition 3.4. Level Order. Given a causal DAG $\mathcal{G}(\mathbf{X}, \mathbf{E})$, its level order is the systematic assignment of levels to variables, beginning with level 0 to the set of variables $\{X_i | pa(X_i) = \emptyset\}$. Subsequently, each remaining variable is assigned a level such that for each variable at a given level i , the length of the longest directed path from one/more variables in level 0 is i .

Proposition 3.1. Let the true causal DAG be $\mathcal{G}(\mathbf{X}, \mathbf{E})$ with ground-truth adjacency matrix A . Consider a procedure to estimate a graph $\hat{\mathcal{G}}$ by querying a Perfect Expert (as in Def. 3.3) with pairwise queries X_i, X_j with auxiliary set \mathbf{O}_{ij} , followed by subsequent aggregation of predicted edges from each query (i.e. from a total of $|\mathbf{X}|C_2$ queries). The causal order of the graph $\hat{\mathcal{G}}$ thus estimated is correct, i.e. $D_{top}(\pi(\hat{\mathcal{G}}), A) = 0$ for all values of the sets \mathbf{O}_{ij} . As a corollary, the causal graph thus estimated can however have errors. In other words, when $\mathbf{O}_{ij} = \emptyset \forall i, j$, $D_{top}(\pi(\hat{\mathcal{G}}), A) = 0$ whereas Structural Hamming Distance (SHD) between \mathcal{G} and $\hat{\mathcal{G}} = \sum_{i=1}^{|\mathbf{X}|} |de(X_i)| - |ch(X_i)|$.

Figure 3 illustrates the result of the proposition using empirical simulation. Given a fixed number of nodes, we sample a graph at random as the ‘ground truth’ and then consider all graph orientations of the same size (number of nodes) such that $D_{top} = 0$ w.r.t. the ground truth graph. These are potentially the graphs outputted by a Perfect Expert with different values of the auxiliary set \mathbf{O} . For this set of graphs, we compute SHD w.r.t the ground truth graph. Notice the variance in SHD, despite D_{top} being 0. For graphs with six nodes, SHD can vary from 0 to 14 even as $D_{top} = 0$.

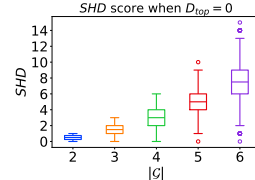


Figure 3: Variability of SHD for various graph sizes with $D_{top} = 0$ within each graph.

The above observations indicate that SHD can be high even when we obtain information from a Perfect Expert, but D_{top} is always 0. This result is of significance since most estimated graphs (including those that are LLM-generated (Ban et al., 2023b; Long et al., 2023)) are evaluated using graph metrics such as SHD. Rather the graph, it motivates us to posit the use of causal order as a more accurate output interface for experts’ domain knowledge, since it allows objective evaluation of the expert’s output using the topological divergence metric (Defn 3.2).

3.2 DOWNSTREAM UTILITY OF CAUSAL ORDER: DISCOVERY AND EFFECT INFERENCE

While the causal order is a more stable measure of experts’ knowledge than the full graph, a natural question is whether it is a useful measure by itself too. We now show the utility of causal order for effect estimation and causal discovery, which are also supported strongly by our experimental results in Sec 5. Specifically, we show that causal order is sufficient to find a valid backdoor set and D_{top} is an ideal metric to minimize for effect estimation, assuming no latent confounders. Effect estimation error correlates more with topological divergence than it does with SHD. Causal order is also useful as a prior or constraint to increase accuracy of graph discovery algorithms.

Correct topological order is necessary and sufficient for finding a valid backdoor set. We first present the (known) result that a correct causal order is sufficient for identifying a backdoor set. We assume there are no unobserved variables in the underlying causal graph.

Proposition 3.2. (Pearl, 2009; Cinelli et al., 2022) Under the no latent confounding assumption, for a pair of treatment and target variables (X_i, X_j) in a DAG \mathcal{G} , $\mathbf{Z} = \{X_k | \pi_k < \pi_i\}$ is a valid adjustment set relative to (X_i, X_j) for any topological order π of \mathcal{G} .

Proofs of all propositions are provided in Appendix § B. Propn 3.2 states, in simple words, that all variables that precede the treatment variable in a topological order π of \mathcal{G} constitute a valid adjustment set. Note that the set \mathbf{Z} may contain variables that are not necessary to adjust for (e.g., ancestors of only treatment or target variables). For statistical efficiency purposes, ancestors of the target variable are helpful for precise effect estimation, whereas ancestors of treatment variable can be harmful (Cinelli et al., 2022). However, asymptotically, as the number of data points increases, such variables do not have any impact on the estimation.

We now show that D_{top} is an optimal metric to minimize for effect estimation. That is, D_{top} being 0 for a topological order is equivalent to obtaining the correct backdoor adjustment set using

270 Proposition 3.2. And if $D_{top} \neq 0$, there exists some treatment-target pair whose backdoor set is not
 271 correctly identified.

272 **Proposition 3.3.** For an estimated topological order $\hat{\pi}$ and a true topological order π of a causal
 273 DAG \mathcal{G} with the corresponding adjacency matrix A , $D_{top}(\hat{\pi}, A) = 0$ iff $\mathbf{Z} = \{X_k | \hat{\pi}_k < \hat{\pi}_i\}$ is a
 274 valid adjustment set relative to (X_i, X_j) , $\forall \pi_i < \pi_j$.
 275

276 Empirically, the correlation of D_{top} with effect estimation is shown in App. D for common bnlearn
 277 datasets. As long as D_{top} is zero, changing the graph has no impact on effect estimation error.
 278

279 **Topological order can improve accuracy of graph discovery algorithms.** Constraints implied by
 the topological order can be used to reduce the search space for discovery algorithms. For instance, if
 280 $X_i \prec X_j$ in the order, then X_i cannot be a descendant of X_j in the corresponding causal graph.
 281

282 *Using causal order with Constraint-Based Discovery Methods.* Constraint-based causal discovery
 algorithms usually return a Completed Partially Directed Acyclic Graph (CPDAG), from which
 283 a Markov equivalence class of graphs can be obtained. However, not all edges in a CPDAG are
 284 oriented. Given a CPDAG from a constraint-based algorithm like PC (Spirites et al., 2000), we use
 285 the causal order $\hat{\pi}$ obtained from experts to orient the undirected edges, similar to the algorithm
 286 from Meek (1995). Iterating over undirected edges, we first check if the nodes of that edge occur
 287 in $\hat{\pi}$. If yes, we orient the edge according to $\hat{\pi}$. Since it is possible that the causal order obtained
 288 from querying experts may not include some nodes (isolated nodes), if either (or both) nodes of
 289 the undirected edge are not in $\hat{\pi}$, we query a superior expert (e.g. oracle) (see Sec 4) to finalize a
 290 direction between the pair. Algorithm 1 (Appendix C) outlines the specific steps for this integration.
 291

292 *Using causal order with score-based discovery methods.* Score-based methods like CaMML (Wal-
 lace et al., 1996) allow the specification of prior constraints which are respected while obtaining the
 293 complete graph. We hence utilize the causal order $\hat{\pi}$ obtained from experts as a level order prior (Defn
 294 3.4) to such methods. We handle any cycles in the expert’s output by assigning all nodes in a cycle to
 295 the same level. The approach is similar to an LLM-prior approach by Ban et al. (2023b) where the
 296 output of LLM and a score-based method are combined using an ancestral constraint. This approach
 297 also allows us to provide a prior probability to control the influence of prior on the discovery method.
 298 Algorithm 2 (Appendix C) outlines the specific steps for this integration.
 299

300 4 OBTAINING A CAUSAL ORDER FROM IMPERFECT EXPERTS

301 If we assume a Perfect Expert, then aggregating edge responses from the standard pairwise
 302 prompt (Kiciman et al., 2023) can yield an accurate order. However, in practice, LLMs are im-
 303 perfect experts and their answers can contain unpredictable errors. As a result, aggregating responses
 304 from pairwise prompt leads to many cycles in the final graph (see Sec. 5, Table 3), which in turn
 305 implies that the causal order is undefined. In this section, we propose two ways to reduce the errors
 306 made by an imperfect expert such as LLMs, motivated by Prop. 3.1 that showed that adding additional
 307 context may help an expert avoid creating unnecessary edges. First, we consider strategies to add
 308 auxiliary context in the pairwise prompt. Second, we propose a strategy that adds dynamic context to
 309 each variable pair by iterating over all triplets of variables.

310 4.1 ENHANCING ACCURACY OF PAIRWISE PROMPT

311 One way to avoid cycles is to make the pairwise prompt more robust. Beyond the standard pairwise
 312 prompt that asks the expert to identify the causal relationship between a pair of variables (Kiciman
 313 et al., 2023), we consider the following strategies to add contextual information (see Appendix F).
 314

- 315 • *Iterative Context.* Here we provide the previously oriented pairs as context in the query while
 316 iteratively prompting for next pair.
- 317 • *One-hop Iterative Context.* Providing all previously oriented pairs can become prohibitive for large
 318 graphs. Therefore, in this setting, we limit the provided information to the already oriented edges
 319 connecting the node pair under inspection with their adjacent neighbors. Specifically, we only
 supply the orientation details for the current node pair and their neighboring nodes.
- 320 • *Chain-of-Thought (+In-context Learning).* Here we include names of all variables in the graph as
 321 additional context. Based on recent results on providing in-context examples in LLM prompts for
 322 various tasks (Brown et al., 2020), here we include examples of the ordering task (viz. node pairs
 323 and their correct causal ordering), before asking the question about the given nodes. Please see
 Appendix § F for more details on the implementation.

4.2 THE TRIPLET METHOD FOR PROMPTING LLMs

Rather than providing a pair of variables, another way is to provide a larger set of nodes in a prompt and ask LLM to obey the acyclicity constraint while providing the edges among them. The number of total prompts used for a graph with size $|V|$ would be $O(|V|^k)$ where k is the size of the subset included in each prompt. In addition, LLM’s accuracy is known to reduce as the query prompt becomes more complex (Levy et al., 2024). Therefore, while the set of nodes can be of any size, we decide to go with triplet-based prompts as they allow for adding more context with minimal increase in prompt complexity and the total number of LLM calls. Moreover, empirically, we did not see a noticeable improvement in accuracy when moving from a triplet to quadruplet prompt (see Table A9).

In effect, we move from $O(|V|^2)$ calls to $O(|V|^3)$ LLM calls. A side-benefit is that for each pair of nodes, we have $n - 1$ answers from the LLM, each considering a different auxiliary node as context. To aggregate the final graph, we take majority vote on the answers from each edge, further leading to robustness. To resolve ties, we use a high-cost expert, as described below. Finally, we extract the causal order from this graph.

1. From a given set of graph nodes, we generate all possible triplets of nodes.
2. We query the expert to orient nodes of each triplet group to form a DAG representing the causal relationship between the triplet’s nodes. This results in multiple acyclic mini-graphs representing causal relationships for each triplet group.
3. Once we have DAGs for each triplet, we focus on merging them. This is done in two steps: (i) We iterate over all node pairs, and for each combination we obtain a majority vote on the orientation between them across all triplets containing the node pair; (ii) In case of a conflict (or a tie in the majority vote) among the three possible edge orientations ($A \rightarrow B$; $B \rightarrow A$; No edge between A and B), we resort to a high-cost expert for tie-breaking.
4. Finally, a causal order is extracted from the merged graph.

Our triplet prompt additionally use in-context examples and the chain-of-thought strategy from the pairwise setup. An example prompt is shown in Table A24.

Theoretical Analysis. Next, we analyze the triplet strategy for its impact on predicting incorrect edges. By enforcing the acyclicity constraint for each triplet, the triplet prompt avoids errors that a pairwise prompt may make¹. We begin by defining (imperfect) ϵ -experts, as in (Long et al., 2023). For ease of exposition, we define the ϵ -expert to have error probability *exactly* equal to ϵ ; this could however be generalized to have error probability at most ϵ .

Definition 4.1 (ϵ -Experts). *Given two nodes A and B of a graph and three options of the causal relationship between them: (i) $A \rightarrow B$, (ii) $A \leftarrow B$, and (iii) no edge between A and B (denoted as $[c_1, c_2, c_3]$), an expert \mathcal{E} queried for the causal relationship between A and B is said to be an ϵ -expert (denoted as \mathcal{E}_ϵ) if the probability of making an error in the prediction of the causal relationship between A and B is ϵ , where $\epsilon \in (0, 1)$.*

Proposition 4.1. *Given two nodes A and B of an underlying causal graph, access to an ϵ -expert \mathcal{E}_ϵ that doesn’t produce any cycles in the predicted causal graph (see Assm B.1 for formal statement) and renormalizes the probability in case an option is not available (see Assm B.2 for formal statement), let $C \neq A \neq B$ be any other node in the graph. If \mathcal{E}_ϵ predicts causal relationship between all pairs of nodes sequentially, the marginalized probability that \mathcal{E}_ϵ makes an error in predicting the causal relationship between A and B , after it has already predicted the causal relationships between (C, A) and (C, B) , is less than ϵ , where marginalization is over all possible causal graphs that can be formed between A, B and C , with each of such graphs being equally likely.*

In other words, a querying strategy using triplets will have error probability $< \epsilon$ over determining the causal relationship between A and B than a pairwise strategy (proof in Appendix B). Still, some cycles may be produced in the aggregated global graph, hence we use a cycle removal algorithm inspired from (Zheng et al., 2018) in the third step of our triplet method. For every edge, we leverage the votes from the triplet prompts to establish a probability distribution over edge orientations. We use this to compute entropy for each edge, removing those with higher entropy (lower confidence). To minimize D_{top} , we prune edges with entropy below the mean of all entropies.

¹For imperfect experts, we have the option of enforcing the acyclicity constraint by removing any cycles from their triplet output. However, we find that this step is not needed for GPT-3.5 and GPT-4 as they follow the acyclicity constraint with high accuracy.

5 EXPERIMENTS AND RESULTS

Datasets. To validate the usefulness of the proposed framework, we perform experiments across multiple benchmark datasets from the BNLearn repository (Scutari & Denis, 2014): Earthquake, Cancer, Survey, Asia, Asia modified (Asia-M), and Child. Asia-M is derived from Asia by removing the node *either* since it is not a node with a semantic meaning (see Appendix § F for details). To study memorization in the context of our experiments and to test our proposed solutions impact on densely connected complex networks, we use recently proposed, less popular datasets that require nuanced medical domain understanding: (i) **Neuropathic**: A medium-sized subset graph from a relatively less popular Neuropathic dataset (Tu et al., 2019) (see Appendix Fig A8). (ii) **Alzheimers**: This graph (refer Figure A9) provides comprehensive features (such as ventricular volume, brain volume, APOE4, etc) to study the clinical and phenotype of Alzheimer’s disease (Abdulaal et al., 2024). It was curated by a consensus across human experts. (iii) **Covid-19**: This graph, curated by medical experts, models the initial pathophysiological process of SARS-CoV-2 in the respiratory system which involves outlining the various pathways from viral infection to key complications (refer Figure A10). Orienting this graph requires understanding of how nodes like Pulmonary capillary leakage, systemic inflammatory response, Viremia and more influence each other (Mascaro et al., 2022).

Imperfect Experts. We consider two types of imperfect experts: *LLMs* and *human annotators*.

Human Annotation: Description and Results. We considered 15 human annotators, each with undergrad-level training in STEM but no formal experience in causality. Each annotator was randomly allotted a graph for both pairwise and triplet query strategies while ensuring no annotator got the same graph to query with both strategies. To get an estimate of the upper bound of human performance, for resolving tie-breaking conflicts in the triplet method, we used a ground truth-based oracle (proxy for a human domain expert).

Results: Even with human annotators, graphs like *Survey* and *Asia-M* result in cycles when queried pairwise. However, no cycle formations were observed across annotators when they were queried to orient causal graphs using the triplet strategy. Also, the triplet strategy showed consistently low D_{top} across all human outputs. This highlights the effectiveness of triplet over other types of imperfect experts beyond LLMs.

LLM-Based: Description and Results. For LLM-based expert assessment, GPT-3.5-turbo was used as the imperfect expert and GPT-4 for tie-breaking. To understand the effect of model size, we also evaluate the pairwise and triplet methods on Phi-3 (3.8B parameters) (Abdin, 2024) and Llama3 (8B parameters) (Dubey, 2024) which are smaller models than GPT-3.5-turbo and GPT-4.

Results: We first present the accuracy of obtaining causal order using our triplet-based approach over other pairwise query strategies. Subsequently, we present the results of using the causal order obtained from imperfect experts to downstream tasks such as causal discovery and effect inference.

Results with Pairwise Optimizations: Tables A5 and A6 present the performance of various pairwise optimization strategies, as detailed in Sec 4.1. The results show that our pairwise variations improve graph discovery but still fall short. While strategies like CoT offer some gains over the base pairwise method, they often produce cycles, especially in larger graphs like Child. These findings emphasize that pairwise optimization does not yield cycle-free graphs, unlike our triplet’s consistent results.

Results with Triplet vs Pairwise Query Strategies: Table 3 compares triplet and pairwise query strategies across benchmark datasets using metrics like D_{top} , SHD, Cycles, IN, and TN, with LLMs (GPT-3.5-turbo) as an imperfect expert. Triplet consistently outperforms the best pairwise approach (our proposed CoT baseline) and shows a larger performance gap when compared to the standard pairwise strategy. Full pairwise results are available in Appendix D.4. Except for the Earthquake and Survey datasets, the pairwise (CoT) prompt results in a null D_{top} due to cycle formation. For larger graphs like Child, the difference is more pronounced, with higher cycle counts and SHD for the pairwise base approach. While CoT improves upon this, cycles persist. Results on the Neuropathic dataset further confirm that pairwise consistently produces cycles, while triplet always yields cycle-free graphs.

Results with GPT-4 Pairwise Querying: To assess the impact of using a more advanced model like GPT-4 for pairwise querying, we analyze its performance on various benchmarks. Despite the model’s capabilities, we observe a consistently high number of cycles, indicating that simply upgrading the model does not resolve the issue if the querying strategy remains unchanged (see Table A7). For e.g., for bigger graphs like Neuropathic and Child, the number of cycles remain consistently high even after replacing a weaker model like GPT-3.5-turbo with a stronger GPT-4. Even in complex medical domain datasets (e.g. COVID-19, Alzheimer’s), pairwise prompting leads to cycle formation when using GPT-4 as an expert, underscoring the limitations of this strategy and the ineffectiveness

Dataset	Metric	Pairwise	Triplet
Using Human Annotators			
Earthquake	D_{top}	0	0
	SHD	4.67	1.67
	Cycles	0	0
	IN	0	0.33
Survey	D_{top}	-	0
	SHD	6.33	3.67
	Cycles	0.67	0
	IN	0.67	0
Cancer	D_{top}	0	0
	SHD	4.33	3.67
	Cycles	0	0
	IN	0.67	0
Asia-M	D_{top}	-	1.33
	SHD	11.67	11.33
	Cycles	3	0
	IN	0	0

Table 1: Experiments with non-expert human annotators show that the triplet method consistently produces the most robust final graph, demonstrating its effectiveness with LLM-based experts.

Dataset	Metric	Pairwise GPT-4	Triplet Phi-3	Triplet Llama3
Asia	D_{top}	1	0	2
	SHD	18	13	17
	Cycles	0	0	0
	IN/TN	0/5	1/5	0/5
Alzheimers	D_{top}	-	7	5
	Cycles	1	0	0
	IN/TN	0/11	0/11	1/11
	IN/TN	0/20	0/20	0/20
Child	D_{top}	-	17	12
	SHD	148	69	129
	Cycles	$\gg 10k$	0	0
	IN/TN	0/20	0/20	0/20

Table 2: Comparison of GPT-4 Pairwise Base with Phi-3/Llama3 using the Triplet method, showing how smaller models outperform GPT-4 by producing cycle-free graphs. This underscores the importance of the triplet strategy, regardless of the expert model used.

Dataset	PC	SCORE	ICA LINGAM	Direct LINGAM	NOTEARS	CaMML	Ours (PC+LLM)	Ours (CaMML+LLM)	Ours (PC+Human)	Ours (CaMML+Human)
$N = 250$	Earthquake	0.16±0.28	4.00±0.00	1.00±0.00	1.00±0.00	1.00±0.00	0.00±0.00	0.00±0.00	0.00±0.00	1.00±0.00
	Cancer	0.00±0.00	3.00±0.00	2.00±0.00	2.00±0.00	2.00±0.00	0.00±0.00	0.00±0.00	0.00±0.00	0.00±0.00
	Survey	0.50±0.00	4.00±0.00	2.00±0.00	4.00±0.00	4.00±0.00	0.00±0.00	3.33±0.94	0.00±0.00	0.00±0.00
	Asia	2.00±0.59	7.00±0.00	3.33±0.47	1.00±0.00	3.00±0.00	1.85±0.58	1.00±0.00	0.97±0.62	N/A
	Asia-M	1.50±0.00	6.00±0.00	1.00±0.00	3.00±0.00	3.00±0.00	1.00±0.00	1.00±0.00	1.71±0.45	1.00±0.00
	Child	5.75±0.00	12.0±0.00	14.33±0.47	16.0±0.00	14.0±0.00	3.00±0.00	4.00±0.00	3.53±0.45	N/A
	Neuropathic	4.00±0.00	6.00±0.00	13.0±6.16	10.0±0.00	9.00±0.00	10.4±1.95	3.00±0.00	5.00±0.00	N/A
$N = 10000$	Earthquake	0.00±0.00	4.00±0.00	3.00±0.00	3.00±0.00	1.00±0.00	0.00±0.00	0.00±0.00	0.00±0.00	0.00±0.00
	Cancer	2.00±0.00	3.00±0.00	3.00±0.00	3.00±0.00	2.00±0.00	0.60±0.80	2.00±0.00	0.00±0.00	0.00±0.00
	Survey	2.00±0.00	4.00±0.00	5.00±0.00	5.00±0.00	3.00±0.00	3.60±1.35	2.00±0.00	1.83±0.00	2.00±0.00
	Asia	1.5±0.00	4.00±0.00	6.00±0.00	4.40±1.35	3.00±0.00	1.40±0.48	0.00±0.00	0.34±0.47	N/A
	Asia-M	1.00±0.00	4.00±0.00	8.00±0.00	4.80±0.39	3.00±0.00	2.00±0.00	0.00±0.00	0.00±0.00	0.00±0.00
	Child	6.00±3.04	3.00±0.00	12.2±1.46	11.6±0.48	14.4±0.48	2.80±0.84	5.00±2.64	1.00±0.00	N/A
	Neuropathic	10.00±0.00	6.00±0.00	1.00±0.00	10.0±0.00	10.0±0.00	3.00±0.00	10.00±0.00	1.00±0.00	N/A

Table 4: Comparison with causal discovery methods, showing mean and std dev of D_{top} over 3 runs. (For the Neuropathic subgraph (1k samples), PC Algorithm returns cyclic graphs in the MEC). Human experiments not conducted for Neuropathic, Child (due to feasibility issues) and Asia; hence rows marked as N/A.

of solely improving expert quality.

Results with Small LMs: Our ablation study on Phi-3 and Llama3-8b with GPT-4 as a tie-breaker shows that triplet consistently outperforms pairwise, producing cycle-free graphs for both small and large-scale graphs with high interconnections (see Table A8). Pairwise (both base and CoT) often returns cycles, even for small graphs like Asia, with performance degrading as graph size and interconnections increase. Triplet, on the other hand, consistently yields cycle-free graphs with low D_{top} values. Remarkably, as shown in Table 3, the triplet pipeline for smaller LMs outperforms pairwise querying with large models like GPT-4, particularly for complex networks, demonstrating better robustness and more efficient use of model capabilities.

Table 3: Results using GPT-3.5-Turbo. Performance of triplet method, best performing pairwise query strategy (Chain of Thought), standard pairwise technique (Base) on multiple benchmark datasets across diff metrics: D_{top} , SHD, (Num of) Cycles, IN, TN. When number of cycles > 0 , $\hat{\pi}$ cannot be computed, hence D_{top} is given by ‘-’. While CoT method shows improvement over base pairwise, triplet still emerges as the overall winner across all datasets. Triplet consistently outperforms the pairwise strategy across metrics & datasets, especially by significant amounts on larger graphs like *Child* and *Neuropathic*.

Dataset	Metric	Pairwise (Base)	Pairwise (CoT)	Triplet
Using LLM				
Earthquake	D_{top}	0	0	0
	SHD	7	4	4
	Cycles	0	0	0
	IN/TN	0/5	0/5	0/5
Survey	D_{top}	3	1	0
	SHD	12	9	9
	Cycles	0	0	0
	IN/TN	0/6	2/6	0/6
Cancer	D_{top}	0	-	1
	SHD	6	-	6
	Cycles	0	-	0
	IN/TN	0/5	-	0/5
Asia-M	D_{top}	-	-	1
	SHD	15	13	11
	Cycles	7	1	0
	IN/TN	0/7	0/7	0/7
Child	D_{top}	-	-	1
	SHD	177	138	28
	Cycles	$\gg 3k$	$\gg 500$	0
	IN/TN	0/20	0/20	0/20
Covid	D_{top}	-	0	0
	SHD	41	27	30
	Cycles	$\gg 1000$	0	0
	IN/TN	0/20	0/20	0/20
Alzheimers	D_{top}	-	6	4
	SHD	42	26	28
	Cycles	684	0	0
	IN/TN	0/20	0/20	0/20
Neuropathic	D_{top}	-	-	3
	SHD	212	64	24
	Cycles	$\gg 5k$	5	0
	IN/TN	0/22	0/22	13/22

Study on Downstream Applications: Causal Discovery. Table 4 presents the D_{top} results of using the causal order obtained from the triplet method (both using LLMs and humans) to assist causal discovery methods. We compare our overall approach using triplet queries with well-known causal discovery methods: PC (Spirtes et al., 2000), SCORE (Rolland et al., 2022), ICA-LiNGAM (Shimizu et al., 2006), Direct-LiNGAM (Shimizu et al., 2011), NOTEARS (Zheng et al., 2018), and Causal discovery via minimum message length (CaMML) (Wallace et al., 1996) across five different sample sizes: 250, 500, 1000, 5000, 10000 (complete results in Appendix Table A3). Among the discovery algorithms, we find that PC and CaMML perform the best, with the lowest D_{top} across all datasets. We hence studied 4 variants of using the causal order with discovery algorithms: PC+Human, CaMML+Human, PC+LLM, and CaMML+LLM. The results show that using expert-provided causal order improves D_{top} across our experiments consistently. Specifically, the improvement (reduction) in D_{top} when using our approach is larger at lower sample sizes. This indicates that obtaining causal order from imperfect experts like humans and LLMs can help with causal discovery in limited sample settings. Overall, these results show that expert output can significantly improve the accuracy of existing causal discovery algorithms. To further investigate the potential impact of memorization, since BNLearn datasets are widely used and the model may have encountered them during pretraining, we also evaluate its performance on the medium size subset of Neuropathic dataset used for pain diagnosis. The result trend in the Table show how triplet consistently leads to low D_{top} with 0 cycles.

Study on Downstream Applications: Causal Effect Inference. Table 5 presents results of a similar experimental study that uses the causal order obtained from our LLMs to compute average causal effect (ACE). We report the error in ACE ϵ_{ACE} across the same set of methods and datasets as above. The obtained causal order shows unanimous improvement in performance across the studies, especially when using the causal order from CaMML+LLM.

Dataset	Metric: ϵ_{ACE} (Treatment, Target)	PC	SCORE	ICA LiNGAM	Direct LiNGAM	NOTEARS	CaMML	Ours (PC+LLM)	Ours (CaMML+LLM)
Earthquake	(JohnCalls,alarm)	0.00 ± 0.00	0.85 ± 0.02	0.63 ± 0.10	0.63 ± 0.10	0.21 ± 0.12	0.08 ± 0.03	0.00 ± 0.00	0.00 ± 0.00
Cancer	(dyspnoea,cancer)	0.20 ± 0.01	0.30 ± 0.00	0.30 ± 0.01	0.30 ± 0.01	0.18 ± 0.02	0.06 ± 0.00	0.30 ± 0.00	0.00 ± 0.00
Survey	(T,E)	0.02 ± 0.00	0.04 ± 0.00	0.05 ± 0.01	0.05 ± 0.01	0.03 ± 0.00	0.03 ± 0.00	0.02 ± 0.01	0.01 ± 0.01
Asia	(smoke,dyspnoea)	0.10 ± 0.00	0.09 ± 0.00	0.27 ± 0.03	0.27 ± 0.04	0.14 ± 0.01	0.05 ± 0.00	0.02 ± 0.00	0.00 ± 0.00
Child	(Lung Parench, Lowerbody O2)	0.22 ± 0.01	0.02 ± 0.00	0.52 ± 0.00	0.52 ± 0.00	0.52 ± 0.07	0.01 ± 0.00	0.22 ± 0.00	0.00 ± 0.00

Table 5: Comparison of causal effect inference with existing methods, showing mean and std dev of error in Average Causal Effect (ϵ_{ACE}) of a variable on another, over 3 runs.

	PC	SCORE	ICA LiNGAM	Direct LiNGAM	NOTEARS	CaMML	Ours (PC+LLM)	Ours (CaMML+LLM)
$N = 250$	4.00±0.00	6.00±0.00	13.0±6.16	10.0±0.00	9.00±0.00	10.4±1.95	3.00±0.00	5.00±0.00
$N = 10000$	10.00±0.00	6.00±0.00	1.00±0.00	10.0±0.00	10.0±0.00	3.00±0.00	10.00±0.00	1.00±0.00

Table 6: Performance on causal discovery for the *Neuropathic* dataset subgraph (1k samples), showing mean and std dev of D_{top} over 3 runs.

Cost Estimation Analysis: Pairwise vs Triplet for LLMs: Triplet is a more cost-effective approach, leveraging smaller models for efficiency and reserving larger models only for clash resolution. This reduces LLM inference costs while outperforming pairwise. See Appendix E for a detailed cost comparison. Our results also show that open-source models like Phi-3, when used with triplet, can outperform costly models like GPT-4 under pairwise querying.

6 CONCLUDING DISCUSSION

Obtaining reliable knowledge from imperfect experts is challenging. We presented causal order as a suitable output interface to elicit causal knowledge from imperfect experts like LLMs and human annotators. Compared to the full graph, we showed that causal order is a more stable quantity to elicit from imperfect experts since it avoids making a distinction between direct and indirect effects. We also proposed a novel triplet-based method to query experts for obtaining the causal order. Empirical results show the benefits of triplet method in avoiding cycles in the causal order and in improving accuracy of downstream discovery and effect inference tasks.

Limitations. While causal order may be sufficient for downstream causal tasks like effect estimation, it may not be sufficient for tasks like counterfactual generation and root cause analysis (Janzing et al., 2019) that require the graph structure for estimating functional equations. In such cases, a viable method may be to obtain causal order from an expert and then use it as a prior /constraint for existing discovery methods to obtain the full causal graph.

540 ETHICAL IMPACT AND REPRODUCIBILITY

541
542 *Ethical Statement.* All datasets used in our work are publicly available and are accurate to the best
543 of our knowledge. We made best efforts to compare against contemporary benchmarks in a fair
544 manner. There may be no direct harmful impact, especially considering our causal order is only a
545 pre-processing steps for downstream algorithms. However, since LLMs may be used in our approach,
546 suitable prudence may be necessary to avoid ill-effects in applications.

547 *Reproducibility.* Our methods are fairly straightforward, and implementation details are already
548 included in our paper descriptions. We will release our code publicly on acceptance.
549

550 REFERENCES

551
552 Abdin. Phi-3 technical report: A highly capable language model locally on your phone, 2024. URL
553 <https://arxiv.org/abs/2404.14219>.

554
555 Ahmed Abdulaal, adamos hadjivasilou, Nina Montana-Brown, Tiantian He, Ayodeji Ijshakin, Ivana
556 Drobnjak, Daniel C. Castro, and Daniel C. Alexander. Causal modelling agents: Causal graph
557 discovery through synergising metadata- and data-driven reasoning. In *The Twelfth International
558 Conference on Learning Representations*, 2024. URL [https://openreview.net/forum?
559 id=pAoqRlTBtY](https://openreview.net/forum?id=pAoqRlTBtY).

560 Alessandro Antonucci, Gregorio Piqué, and Marco Zaffalon. Zero-shot causal graph extrapolation
561 from text via llms. *arXiv preprint arXiv:2312.14670*, 2023.
562

563 Taiyu Ban, Lyuzhou Chen, Derui Lyu, Xiangyu Wang, and Huanhuan Chen. Causal structure learning
564 supervised by large language model. *arXiv preprint arXiv:2311.11689*, 2023a.

565 Taiyu Ban, Lyvzhou Chen, Xiangyu Wang, and Huanhuan Chen. From query tools to causal
566 architects: Harnessing large language models for advanced causal discovery from data. *arXiv
567 preprint arXiv:2306.16902*, 2023b.
568

569 Tom B. Brown, Benjamin Mann, Nick Ryder, Melanie Subbiah, Jared Kaplan, Prafulla Dhariwal,
570 Arvind Neelakantan, Pranav Shyam, Girish Sastry, Amanda Askell, Sandhini Agarwal, Ariel
571 Herbert-Voss, Gretchen Krueger, Tom Henighan, Rewon Child, Aditya Ramesh, Daniel M. Ziegler,
572 Jeffrey Wu, Clemens Winter, Christopher Hesse, Mark Chen, Eric Sigler, Mateusz Litwin, Scott
573 Gray, Benjamin Chess, Jack Clark, Christopher Berner, Sam McCandlish, Alec Radford, Ilya
574 Sutskever, and Dario Amodei. Language models are few-shot learners. *CoRR*, abs/2005.14165,
575 2020.

576 Kristy Choi, Chris Cundy, Sanjari Srivastava, and Stefano Ermon. Lmpriors: Pre-trained language
577 models as task-specific priors, 2022. URL <https://arxiv.org/abs/2210.12530>.

578
579 Carlos Cinelli, Andrew Forney, and Judea Pearl. A crash course in good and bad controls. *Sociological
580 Methods & Research*, pp. 00491241221099552, 2022.

581 Kai-Hendrik Cohrs, Emiliano Diaz, Vasileios Sitokonstantinou, Gherardo Varando, and Gustau
582 Camps-Valls. Large language models for constrained-based causal discovery. In *AAAI 2024
583 Workshop on "Are Large Language Models Simply Causal Parrots?"*, 2023.
584

585 Anthony C. Constantinou, Zhigao Guo, and Neville K. Kitson. The impact of prior knowledge on
586 causal structure learning. *Knowledge and Information Systems*, 65(8):3385–3434, 2023.

587
588 Dubey. The llama 3 herd of models, 2024. URL <https://arxiv.org/abs/2407.21783>.

589 Uzma Hasan and Md Osman Gani. Kcrl: A prior knowledge based causal discovery framework with
590 reinforcement learning. In *Proceedings of the 7th Machine Learning for Healthcare Conference*,
591 2022.
592

593 David Heckerman and Dan Geiger. Learning bayesian networks: a unification for discrete and
gaussian domains. *arXiv preprint arXiv:1302.4957*, 2013.

- 594 Dominik Janzing, Kailash Budhathoki, Lenon Minorics, and Patrick Blöbaum. Causal structure based
595 root cause analysis of outliers, 2019. URL <https://arxiv.org/abs/1912.02724>.
596
- 597 Thomas Jiralerspong, Xiaoyin Chen, Yash More, Vedant Shah, and Yoshua Bengio. Efficient causal
598 graph discovery using large language models. *arXiv preprint arXiv:2402.01207*, 2024.
- 599 Elahe Khatibi, Mahyar Abbasian, Zhongqi Yang, Iman Azimi, and Amir M Rahmani. Alcm:
600 Autonomous llm-augmented causal discovery framework. *arXiv preprint arXiv:2405.01744*, 2024.
601
- 602 Emre Kıcıman, Robert Ness, Amit Sharma, and Chenhao Tan. Causal reasoning and large language
603 models: Opening a new frontier for causality. *arXiv preprint arXiv:2305.00050*, 2023.
- 604 Mosh Levy, Alon Jacoby, and Yoav Goldberg. Same task, more tokens: the impact of input length
605 on the reasoning performance of large language models, 2024. URL [https://arxiv.org/
606 abs/2402.14848](https://arxiv.org/abs/2402.14848).
607
- 608 Stephanie Long, Tibor Schuster, and Alexandre Piché. Can large language models build causal
609 graphs? In *NeurIPS 2022 Workshop on Causality for Real-world Impact*, 2022.
- 610 Stephanie Long, Alexandre Piché, Valentina Zantedeschi, Tibor Schuster, and Alexandre Drouin.
611 Causal discovery with language models as imperfect experts. In *ICML 2023 Workshop on Struc-
612 tured Probabilistic Inference & Generative Modeling*, 2023.
- 613 Steven Mascaro, Yue Wu, Owen Woodberry, Erik P. Nyberg, Ross Pearson, Jessica Ramsay, Ariel
614 Mace, David Foley, Tom Snelling, and Ann E. Nicholson. Modeling covid-19 disease processes by
615 remote elicitation of causal bayesian networks from medical experts. *medRxiv*, 2022. doi: 10.1101/
616 2022.02.14.22270925. URL [https://www.medrxiv.org/content/early/2022/02/
617 17/2022.02.14.22270925](https://www.medrxiv.org/content/early/2022/02/17/2022.02.14.22270925).
618
- 619 Christopher Meek. Causal inference and causal explanation with background knowledge. In
620 *Proceedings of the Eleventh conference on Uncertainty in artificial intelligence*, pp. 403–410,
621 1995.
- 622 Narmada Naik, Ayush Khandelwal, Mohit Joshi, Madhusudan Atre, Hollis Wright, Kavya Kannan,
623 Scott Hill, Giridhar Mamidipudi, Ganapati Srinivasa, Carlo Bifulco, et al. Applying large language
624 models for causal structure learning in non small cell lung cancer. *arXiv preprint arXiv:2311.07191*,
625 2023.
- 626 Rodney T O’Donnell, Ann E Nicholson, Bin Han, Kevin B Korb, Md Jahangir Alam, and Lucas R
627 Hope. Causal discovery with prior information. In *AI 2006: Advances in Artificial Intelligence:
628 19th Australian Joint Conference on Artificial Intelligence, Hobart, Australia, December 4-8, 2006.
629 Proceedings 19*, pp. 1162–1167. Springer, 2006.
630
- 631 Judea Pearl. *Causality*. Cambridge university press, 2009.
- 632 Jonas Peters and Peter Bühlmann. Structural intervention distance for evaluating causal graphs.
633 *Neural computation*, 27(3):771–799, 2015.
634
- 635 Paul Rolland, Volkan Cevher, Matthäus Kleindessner, Chris Russell, Dominik Janzing, Bernhard
636 Schölkopf, and Francesco Locatello. Score matching enables causal discovery of nonlinear additive
637 noise models. In *ICML*, 2022.
- 638 M. Scutari and J.B. Denis. *Bayesian Networks: With Examples in R*. Chapman & Hall/CRC Texts in
639 Statistical Science. Taylor & Francis, 2014.
640
- 641 Shohei Shimizu, Patrik O Hoyer, Aapo Hyvärinen, Antti Kerminen, and Michael Jordan. A linear
642 non-gaussian acyclic model for causal discovery. *JMLR*, 7(10), 2006.
- 643 Shohei Shimizu, Takanori Inazumi, Yasuhiro Sogawa, Aapo Hyvarinen, Yoshinobu Kawahara,
644 Takashi Washio, Patrik O Hoyer, Kenneth Bollen, and Patrik Hoyer. Directlingam: A direct method
645 for learning a linear non-gaussian structural equation model. *JMLR*, 12(Apr):1225–1248, 2011.
646
- 647 Peter Spirtes, Clark N Glymour, and Richard Scheines. *Causation, prediction, and search*. MIT
press, 2000.

648 Masayuki Takayama, Tadahisa Okuda, Thong Pham, Tatsuyoshi Ikenoue, Shingo Fukuma, Shohei
649 Shimizu, and Akiyoshi Sannai. Integrating large language models in causal discovery: A statistical
650 causal approach. *arXiv preprint arXiv:2402.01454*, 2024.

651 Takeshi Teshima and Masashi Sugiyama. Incorporating causal graphical prior knowledge into
652 predictive modeling via simple data augmentation. In *UAI*, pp. 86–96. PMLR, 2021.

653 Ruibo Tu, Kun Zhang, Bo Bertilson, Hedvig Kjellstrom, and Cheng Zhang. Neuropathic pain
654 diagnosis simulator for causal discovery algorithm evaluation. *NeurIPS*, 32, 2019.

655 Chris Wallace, Kevin B Korb, and Honghua Dai. Causal discovery via mml. In *ICML*, volume 96, pp.
656 516–524, 1996.

657 Jason Wei, Xuezhi Wang, Dale Schuurmans, Maarten Bosma, Fei Xia, Ed Chi, Quoc V Le, Denny
658 Zhou, et al. Chain-of-thought prompting elicits reasoning in large language models. *NeurIPS*, 35:
659 24824–24837, 2022.

660 Moritz Willig, Matej Zečević, Devendra Singh Dhami, and Kristian Kersting. Probing for correlations
661 of causal facts: Large language models and causality. 2022.

662 Yuzhe Zhang, Yipeng Zhang, Yidong Gan, Lina Yao, and Chen Wang. Causal graph discovery with
663 retrieval-augmented generation based large language models. *arXiv preprint arXiv:2402.15301*,
664 2024.

665 Xun Zheng, Bryon Aragam, Pradeep K Ravikumar, and Eric P Xing. Dags with no tears: Continuous
666 optimization for structure learning. *NeurIPS*, 31, 2018.

667
668
669
670
671
672
673
674
675
676
677
678
679
680
681
682
683
684
685
686
687
688
689
690
691
692
693
694
695
696
697
698
699
700
701

APPENDIX

In this appendix, we include the following additional information, which we could not include in the main paper due to space constraints:

- Appendix A: Illustration of our triplet query strategy
- Appendix B: Proofs of propositions
- Appendix C: Algorithms to integrate causal order into existing discovery methods
- Appendix D: Additional results, including LLMs used in post-processing for graph discovery and a discussion of triplet vs pairwise query strategies
- Appendix E: More details and examples of our query strategies
- Appendix F: Causal graphs used in our experiments of the datasets

A ILLUSTRATION OF OUR TRIPLET QUERY STRATEGY

We present an intuitive illustration of our overall triplet querying framework to obtain causal order from imperfect experts in Fig A1 below.

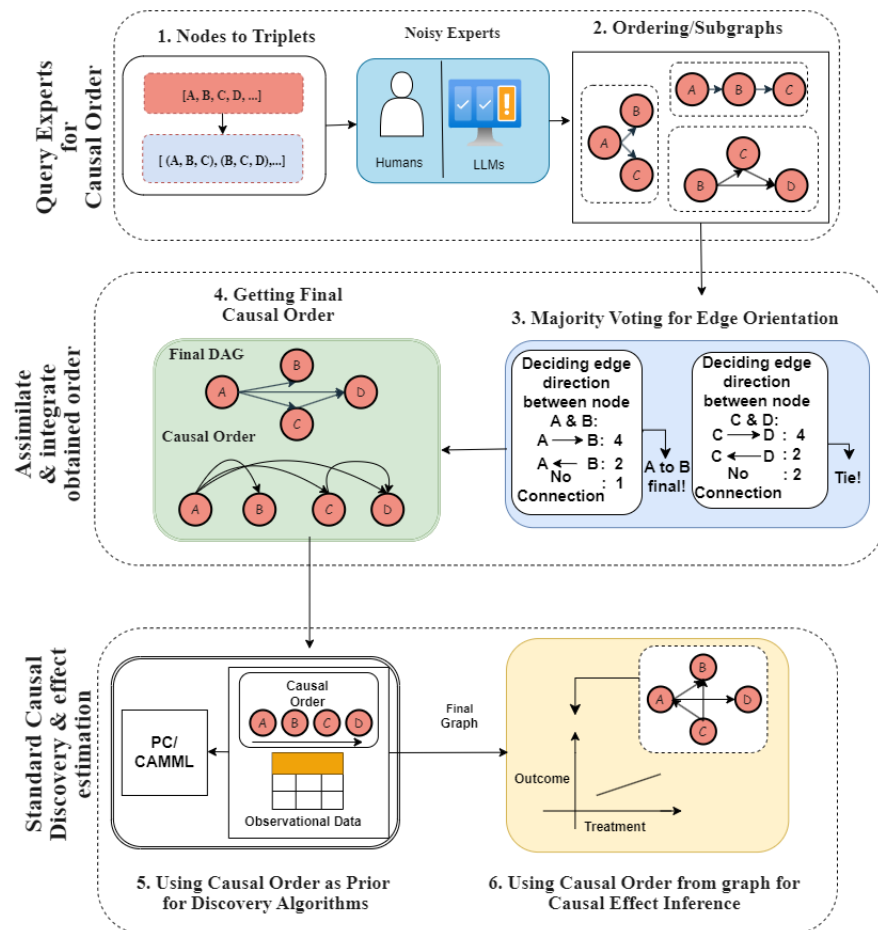


Figure A1: **Leveraging Causal Order from Imperfect Experts.** Our triplet-based querying method infers all three-variable subgraphs from imperfect experts and aggregates them (using majority voting) to produce a causal order. Ties in causal order are broken using a high-cost expert. Expert-generated causal order is integrated with discovery algorithms, before estimating causal effect.

B PROOFS OF PROPOSITIONS

To estimate $\mathbb{E}[X_j | do(X_i = x_i)]$ from observational data, the *backdoor adjustment* formula is used.

Definition B.1. Backdoor Adjustment (Pearl, 2009). Given a DAG \mathcal{G} , a set of variables \mathbf{Z} satisfies the backdoor criterion relative to a pair of treatment and target variables (X_i, X_j) if (i) no variable in \mathbf{Z} is a descendant of X_i ; and (ii) \mathbf{Z} blocks every path between X_i and X_j that contains an arrow into X_i .

Proposition 3.1. Let the true causal DAG be $\mathcal{G}(\mathbf{X}, \mathbf{E})$ with ground-truth adjacency matrix A . Consider a procedure to estimate a graph $\hat{\mathcal{G}}$ by querying a Perfect Expert (as in Def. 3.3) with pairwise queries X_i, X_j with auxiliary set \mathbf{O}_{ij} , followed by subsequent aggregation of predicted edges from each query (i.e. from a total of $|\mathbf{X}|C_2$ queries). The causal order of the graph $\hat{\mathcal{G}}$ thus estimated is correct, i.e. $D_{top}(\pi(\hat{\mathcal{G}}), A) = 0$ for all values of the sets \mathbf{O}_{ij} . As a corollary, the causal graph thus estimated can however have errors. In other words, when $\mathbf{O}_{ij} = \phi \forall i, j$, $D_{top}(\pi(\hat{\mathcal{G}}), A) = 0$ whereas Structural Hamming Distance (SHD) between \mathcal{G} and $\hat{\mathcal{G}} = \sum_{i=1}^{|\mathbf{X}|} |de(X_i)| - |ch(X_i)|$.

Proof. First claim ($D_{top}(\pi(\hat{\mathcal{G}}), A) = 0$): By definition, the Perfect Expert adds new edges that are not present in the true \mathcal{G} , but cannot miss predicting a ground truth edge. This implies that all edges between any two level i, j where $i < j$ that are present in the ground truth graph \mathcal{G} are also present in the estimated graph $\hat{\mathcal{G}}$. Given any two nodes X_1^l and X_2^l with the same level order “ l ” in the true causal graph. Since there is no directed path between X_1^l and X_2^l , the perfect expert will never predict any edge between them (using Def. 3.3). Combining these two observations, the level order of both the graphs $\hat{\mathcal{G}}$ and \mathcal{G} remains the same. Next, we will use the following lemma that states that if the level order of two graphs remains the same then the topological order remains the same thus completing the proof of the first claim.

Lemma B.1. Given two DAG \mathcal{G}_1 and \mathcal{G}_2 have same level order (see Def. 3.4) then there exist two topological order $\pi(\mathcal{G}_1)$ and $\pi(\mathcal{G}_2)$ corresponding to the two DAG s.t. the ordered set $\pi(\mathcal{G}_1) = \pi(\mathcal{G}_2)$.

Proof. Since the level order is the same for both the graphs, all the nodes on a given level “ l ” for both graphs \mathcal{G}_1 and \mathcal{G}_2 are the same. Now, any two nodes on the same level don’t have any edges between them. Thus add all the nodes on the level in the same order to both $\pi(\mathcal{G}_1) = \pi(\mathcal{G}_2)$. Thus when we are done adding the nodes from all the levels in the topological order we get the $\pi(\mathcal{G}_1) = \pi(\mathcal{G}_2)$. \square

Second claim (SHD > 0): Recall that SHD counts the number of missing, falsely detected, and falsely directed edges in the estimated causal graph as compared to the ground truth graph. Since the perfect expert correctly predicts all the ground truth edges, there are no *falsely directed* or *missing* edges in the predicted graph. From Def. 3.3, when queried over all $|\mathbf{X}|C_2$ pairs of nodes the perfect expert will add additional (falsely directed) edges between a node and all its descendants. Thus total number of falsely directed edges = $\sum_{i=1}^{|\mathbf{X}|} |de(X_i)| - |ch(X_i)| = \text{SHD}$. \square

Proposition 3.2. (Pearl, 2009; Cinelli et al., 2022) Under the no latent confounding assumption, for a pair of treatment and target variables (X_i, X_j) in a DAG \mathcal{G} , $\mathbf{Z} = \{X_k | \pi_k < \pi_i\}$ is a valid adjustment set relative to (X_i, X_j) for any topological order π of \mathcal{G} .

Proof. Before starting the proof, we define a confounding variable. A confounder is a variable that should be casually associated with both the treatment and the target variables and is not on the causal pathway between treatment and target. An unmeasured common cause can also be a source of confounding the treatment \rightarrow target relationship. Coming to the proof, we need to show that the set $\mathbf{Z} = \{X_k | \pi_k < \pi_i\}$ satisfies the conditions (i) and (ii) in Defn B.1. For any variable X_k such that $\pi_k < \pi_i$, we have $X_k \notin de(X_i)$ and hence the condition (i) is satisfied. Additionally, for each $X_k \in pa(X_i)$ we have $\pi_k < \pi_i$ and hence $pa(X_i) \subseteq \mathbf{Z}$. Since $pa(X_i)$ blocks all paths from X_i to X_j that contains an arrow into X_i (Peters & Bühlmann, 2015), \mathbf{Z} satisfies condition (ii). \square

Proposition 3.3. For an estimated topological order $\hat{\pi}$ and a true topological order π of a causal DAG \mathcal{G} with the corresponding adjacency matrix A , $D_{top}(\hat{\pi}, A) = 0$ iff $\mathbf{Z} = \{X_k | \hat{\pi}_k < \hat{\pi}_i\}$ is a valid adjustment set relative to (X_i, X_j) , $\forall \pi_i < \pi_j$.

Proof. The statement of proposition is of the form $A \iff B$ with A being “ $D_{top}(\hat{\pi}, A) = 0$ ” and B being “ $\mathbf{Z} = \{X_k | \hat{\pi}_k < \hat{\pi}_i\}$ is a valid adjustment set relative to $(X_i, X_j), \forall i, j$ ”. We prove $A \iff B$ by proving (i) $A \implies B$ and (ii) $B \implies A$.

(i) Proof of $A \implies B$: If $D_{top}(\hat{\pi}, A) = 0$, for all pairs of nodes (X_i, X_j) , we have $\hat{\pi}_i < \hat{\pi}_j$ whenever $\pi_i < \pi_j$. That is, causal order in estimated graph is same that of the causal order in true graph. Hence, from Propn 3.2, $\mathbf{Z} = \{X_k | \hat{\pi}_k < \hat{\pi}_i\}$ is a valid adjustment set relative to $(X_i, X_j), \forall i, j$.

(ii) Proof of $B \implies A$: we prove the logical equivalent form of $B \implies A$ i.e., $\neg A \implies \neg B$, the *contrapositive* of $B \implies A$. To this end, assume $D_{top}(\hat{\pi}, A) \neq 0$, then there will be at least one edge $X_i \rightarrow X_j$ that cannot be oriented correctly due to the estimated topological order $\hat{\pi}$. i.e., $\hat{\pi}_j < \hat{\pi}_i$ but $\pi_j > \pi_i$. Hence, to find the causal effect of X_i on $X_l; l \neq j, X_j$ is included in the back-door adjustment set \mathbf{Z} relative to (X_i, X_l) . Adding X_j to \mathbf{Z} renders \mathbf{Z} an invalid adjustment set because it violates the condition (i) of Defn B.1. \square

Assumption B.1 (DAG Acyclicity). *Given that ϵ -expert \mathcal{E}_ϵ is used to predict a causal graph between a set of nodes, the predicted causal graph is acyclic.*

Assumption B.2 (Error Distribution and Probability Renormalization). *Let $[c_1, c_2, c_3]$ be the three choices for a causal relationship between node A and B (see Def 4.1). Let $P(c_1), P(c_2)$ and $P(c_3)$ be the probability of selecting the corresponding three choices by the ϵ -expert \mathcal{E}_ϵ . We assume that the probability for the two wrong options are equally likely, i.e., equal to $\epsilon/2$. If any constraint \mathcal{T} renders some of the choices as not possible i.e. $P(c_j|\mathcal{T}) = 0$ for some $j \in \{1, 2, 3\}$, then \mathcal{E}_ϵ renormalizes the posterior probability over the other choices, i.e., $P(c_i|\mathcal{T}) = \frac{P(c_i)}{\sum_{j, P(c_j|\mathcal{T}) \neq 0} P(c_j)}$ where the denominator is summed over j s.t. $P(c_j|\mathcal{T}) \neq 0$.*

Proposition 4.1. *Given two nodes A and B of an underlying causal graph, access to an ϵ -expert \mathcal{E}_ϵ that doesn't produce any cycles in the predicted causal graph (see Assm B.1 for formal statement) and renormalizes the probability in case an option is not available (see Assm B.2 for formal statement), let $C \neq A \neq B$ be any other node in the graph. If \mathcal{E}_ϵ predicts causal relationship between all pairs of nodes sequentially, the marginalized probability that \mathcal{E}_ϵ makes an error in predicting the causal relationship between A and B , after it has already predicted the causal relationships between (C, A) and (C, B) , is less than ϵ , where marginalization is over all possible causal graphs that can be formed between A, B and C , with each of such graphs being equally likely.*

Proof. Without any additional constraint, ϵ -expert (\mathcal{E}_ϵ) has “ ϵ ” probability of making incorrect prediction. But in presence of additional constraint, e.g. DAG constraint (see Assm B.1), the probability of error changes and is given by the following lemma:

Lemma B.2. *Suppose we have two nodes A and B and three possible choices $[c_1, c_2, c_3]$ for causal relationship between them i.e $A \rightarrow B, B \rightarrow A$ or no edge between them (not in any particular order). Without loss of generality, let c_3 be the ground truth causal relationship between node A and B . Thus, without any additional constraint, let the probability assigned to each of the three choices by ϵ -expert (\mathcal{E}_ϵ) is $P(c_1) = \epsilon_1, P(c_2) = \epsilon_2$ and $P(c_3) = 1 - \epsilon_1 - \epsilon_2$ respectively where $\epsilon = \epsilon_1 + \epsilon_2$. If due to additional constraint (e.g. acyclicity Assm B.1), one of the incorrect choice gets discarded, say c_1 , then the new probability of selecting the wrong choice (c_2 given by ϵ') is always less than ϵ . However if the correct/ground truth choice is discarded due to this additional constraint the new probability of selecting the wrong choice (c_1 or c_2) is 1. In case, no options are discarded the new probability of choosing the wrong choice remains same i.e ϵ as before.*

Proof. For the case when the correct/ground truth choice i.e c_3 is discarded due to some constraint, the only left out choices are wrong choices i.e. c_1 and c_2 . Thus the probability of making error in selecting the correct choice is 1. Next, for the case when one of the incorrect choice (here c_1 w.l.o.g) is discarded, we are left with one incorrect (c_2) and one correct choice (c_3). From Assm B.2 once a particular option is discarded, the ϵ -expert renormalizes the probability proportional to their initial probability. Thus the new probability ($\tilde{P}(c_2)$) of choosing wrong option c_2 is:

$$\tilde{P}(c_2) = \frac{\epsilon_2}{1 - \epsilon_1 - \epsilon_2 + \epsilon_2} = \frac{\epsilon_2}{1 - \epsilon_1} = \frac{\epsilon/2}{1 - \epsilon/2} = \frac{\epsilon}{2 - \epsilon} \quad (2)$$

where $\epsilon_1 = \epsilon_2 = \epsilon/2$ from Assm B.2. Next, we can show that $\tilde{P}(c_2) < \epsilon$ completing our proof. To have $\tilde{P}(c_2) < \epsilon$ we need:

$$\begin{aligned}\tilde{P}(c_2) &= \frac{\epsilon_2}{1 - \epsilon_1} < \epsilon = \epsilon_1 + \epsilon_2 \\ &\implies \epsilon_2 < \epsilon_1 + \epsilon_2 - \epsilon_1^2 - \epsilon_1\epsilon_2 \\ &\implies \epsilon_1(\epsilon_1 + \epsilon_2 - 1) < 0\end{aligned}\tag{3}$$

which is always true since from Assm B.2 we have $\epsilon_1 > 0$, $\epsilon_2 > 0$ and $1 - \epsilon_1 - \epsilon_2 > 0$. \square

Now, give any three nodes A, B and C , Table A1 summarizes all possible *partially completed* graph (henceforth partial graph) possible between those nodes. Each partially-completed DAG in Table A1 generated more DAG based on the orientation of the node A and B . Specifically, each of the partial graph 1, 2, 3, 4, 5, 7 and 9 generated three graphs ($A \rightarrow B$, $B \rightarrow A$ or no edge between A and B) and partial graph 6 and 8 will give two DAG (one option is not possible to maintain acyclicity constraint). Thus overall we have 25 possible graphs. Our next goal is to show that the marginal probability of choosing the wrong causal relationship for node (A, B) when oriented last among is less than ϵ , where marginalization is over all the causal graph depicted in Table A1 (assuming all graphs are equally likely). The expert \mathcal{E}_ϵ finds the causal relationship sequentially for all the pairs in $\{(C, A), (C, B), (A, B)\}$. We are interested in the case when \mathcal{E}_ϵ finds the causal relationship for pair (A, B) in the end. Let F, S, T (called first, second and third) be three binary random variable and the value 0 represent whether the causal relationship discovered by \mathcal{E}_ϵ for first, second or last/third pair respectively is incorrect and 1 represent it is correct. So the probability of error when finding the causal relationship between node A and B when oriented last/third (denoted by $P(T)$) is given by:

$$\begin{aligned}P(T = 0) &= \sum_{G \in \mathcal{G}} \sum_{S, T \in \{0,1\} \times \{0,1\}} P(G)P(F, S|G)P(T = 0|F, S, G) \\ &= \frac{1}{25} \cdot \sum_{G \in \mathcal{G}} \sum_{S, T \in \{0,1\} \times \{0,1\}} P(F, S|G)P(T = 0|F, S, G)\end{aligned}\tag{4}$$

where \mathcal{G} denotes the set of graphs generated by orienting the causal relationship between A and B for all *partial* graphs in Table A1, $|\mathcal{G}| = 25$ and all the graphs are equally likely, different configuration of (F, S) shows whether the causal relationship between first two pairs (C, A) and (C, B) are correct or not. When orienting the first two pair of nodes i.e (C, A) and (C, B) there is no DAG constraint thus we have:

$$P(F, S) = \begin{cases} \epsilon^2 & \text{when } S = 0, T = 0 \\ \epsilon(1 - \epsilon) & \text{when } S = 0, T = 1 \\ \epsilon(1 - \epsilon) & \text{when } S = 1, T = 0 \\ (1 - \epsilon)^2 & \text{when } S = 1, T = 1 \end{cases}\tag{5}$$

Now based on the graph $G \in \mathcal{G}$ and the setting of S, T , $P(T = 0|F, S, G)$ takes different values. Suppose that the causal relationship between the first two pairs (C, A) and (C, B) are already predicted by the expert. We observe that the DAG acyclicity constraint (Assm B.2) will only change the probability of error for orienting nodes (A, B) ($P(T = 0|F, S, G)$ given by Lemma B.2) when the predicted causal graphs is either $B \rightarrow C \rightarrow A$ or $A \rightarrow C \rightarrow B$ after orienting (C, A) and (C, B) . For all the other predictions of (C, A) and (C, B) , they don't enforce any acyclicity constant for finding the causal relationship between (A, B) , thus, $P(T = 0|F, S, G) = \epsilon$ (from Lemma B.2). Table A2 summarizes of error probability for all the partial graphs in Table A1 ($P(F, S|G)$ and $P(T|F, S, G)$). The first column shows different partial graphs from Table A1. The second column then shows different causal relationships that are possible between the nodes A and B for a particular partial graph. Given one *true orientation* between node A and B we get a final ground truth graph. Thus the third column shows the probability of prediction of structure $A \leftarrow C \rightarrow B$ for a particular true graph and the fourth column shows the probability of making an error in predicting the third causal relationship i.e between (A, B) given the first and second pair (C, A) and $((C, B))$ is already predicted. Similarly, the fifth and sixth columns show the same thing for the predicted structure $A \rightarrow C \rightarrow B$ for each of the ground truth graphs. The partial-graph number 4, 7, 8 is not depicted in the table but the entries for 4th graph is the same as 2nd, 7th is the same as 3rd and 8th is same as 6th due to symmetry in the partial-structure. The value of $\epsilon' = \frac{\epsilon}{2-\epsilon}$ in 4th and 6th column is given by renormalized probability Eq. 2 in Lemma B.2. Substituting the values from Table A2 in Eq. 4

918
919
920
921
922
923
924
925
926
927
928
929
930
931
932
933
934
935
936
937
938
939
940
941
942
943
944
945
946
947
948
949
950
951
952
953
954
955
956
957
958
959
960
961
962
963
964
965
966
967
968
969
970
971

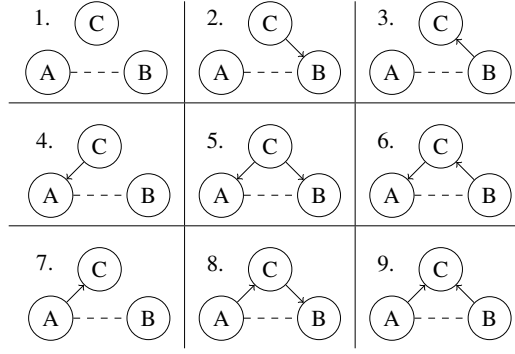


Table A1: All possible causal graph between three variables A, B and C . The dashed arrow represented undecided causal relationship between node A and B . So, the dashed arrow can take one of three choices $A \rightarrow B, A \leftarrow B$ or no edge between A and B . To ensure that the graph is acyclic, some of the graphs above might not allow all three choice for causal relationship between node A and B . Hence the causal-graph 1, 2, 3, 4 and 7 each have three possible graphs and 5, 6, 8 and 9 each have two possible graphs based on the valid choice of causal relationship between A and B that preserves acyclicity constraint. So overall there are 25 possible different causal graph between three variables A, B and C .

and using the value $P(T|F, S, G) = \epsilon$ for the rest of the predicted structure not mentioned in the Table A2 we get:

$$\begin{aligned}
 P(T=0) &= \frac{1}{25} \cdot \left\{ 2 * \frac{\epsilon^2}{4} [2\epsilon' + 1] + [1 - 2 * \frac{\epsilon^2}{4}] \epsilon \right. \\
 &\quad + \left(\left[\frac{\epsilon^2}{4} + \frac{\epsilon(1-\epsilon)}{2} \right] [2\epsilon' + 1] + \left[1 - \frac{\epsilon^2}{4} - \frac{\epsilon(1-\epsilon)}{2} \right] \epsilon \right) * 4 \\
 &\quad + \left(2 * \frac{\epsilon(1-\epsilon)}{2} [2\epsilon' + 1] + \left[1 - 2 * \frac{\epsilon(1-\epsilon)}{2} \right] \epsilon \right) * 2 \\
 &\quad \left. + \left((1-\epsilon)^2 [2\epsilon'] + \frac{\epsilon^2}{4} [\epsilon' + 1] + \left[1 - (1-\epsilon)^2 - \frac{\epsilon^2}{4} \right] \epsilon \right) * 2 \right\} \\
 &= \frac{1}{25} \cdot \left\{ \frac{\epsilon(3\epsilon^2 - 30\epsilon + 52)}{4 - 2\epsilon} \right\}
 \end{aligned} \tag{6}$$

Now we want to show that the error probability for the third pair (A, B) given by the above equation is less than ϵ . For that, we need:

$$\begin{aligned}
 \frac{1}{25} \cdot \left\{ \frac{\epsilon(3\epsilon^2 - 30\epsilon + 52)}{4 - 2\epsilon} \right\} &< \epsilon \\
 3\epsilon^2 + 20\epsilon - 48 &< 0
 \end{aligned} \tag{7}$$

The above inequality is always satisfied since $\epsilon \in (0, 1)$ and $3\epsilon^2 + 20\epsilon - 48$ is always less than 0 in the allowed range of ϵ since the roots of the quadratic equation are $-10/3 - 2\sqrt{61}/3 = -8.5$ and $-10/3 + 2\sqrt{61}/3 = 1.87$. Thus $P(T=0) < \epsilon$ for all values of $\epsilon \in (0, 1)$ completing our proof.

□

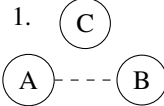
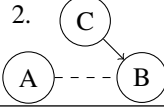
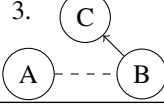
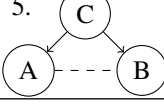
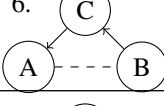
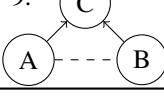
Partial True Graph	True Ori-entation (A, B)	Predicted Orientation in first two steps (F, S)			
		$A \leftarrow C \leftarrow B$		$A \rightarrow C \rightarrow B$	
		$P(F, S G)$	$P(T F, S, G)$	$P(F, S G)$	$P(T F, S, G)$
1. 	no edge $A \rightarrow B$ $A \leftarrow B$	$\left(\frac{\epsilon}{2}\right)^2$	ϵ' 1 ϵ'	$\left(\frac{\epsilon}{2}\right)^2$	ϵ' ϵ' 1
2. 	no edge $A \rightarrow B$ $A \leftarrow B$	$\left(\frac{\epsilon}{2}\right)^2$	ϵ' 1 ϵ'	$\left(\frac{\epsilon}{2}\right)(1 - \epsilon)$	ϵ' ϵ' 1
3. 	no edge $A \rightarrow B$ $A \leftarrow B$	$\left(\frac{\epsilon}{2}\right)(1 - \epsilon)$	ϵ' 1 ϵ'	$\left(\frac{\epsilon}{2}\right)^2$	ϵ' ϵ' 1
5. 	no edge $A \rightarrow B$ $A \leftarrow B$	$\left(\frac{\epsilon}{2}\right)(1 - \epsilon)$	ϵ' 1 ϵ'	$\left(\frac{\epsilon}{2}\right)(1 - \epsilon)$	ϵ' ϵ' 1
6. 	no edge $A \leftarrow B$	$(1 - \epsilon)^2$	ϵ' ϵ'	$\left(\frac{\epsilon}{2}\right)^2$	ϵ' 1
9. 	no edge $A \rightarrow B$ $A \leftarrow B$	$\left(\frac{\epsilon}{2}\right)(1 - \epsilon)$	ϵ' 1 ϵ'	$\left(\frac{\epsilon}{2}\right)(1 - \epsilon)$	ϵ' ϵ' 1

Table A2: Summary of Error Probability for all the partial graphs in Table A1 ($P(F, S|G)$ and $P(T|F, S, G)$): The first column shows different partial graphs from Table A1. The second column then shows different causal relationships that are possible between the nodes A and B for a particular partial graph. Given one true orientation between node A and B we get a final ground truth graph. Now we observed in the proof of Proposition 4.1 (see Proof B), that the error probability for the prediction of causal relationship for the pair (A, B) will only change when the ϵ -expert predicts the the structure $A \leftarrow C \rightarrow B$ or $A \rightarrow C \rightarrow B$ for the pair of nodes (C, A) and (C, B) for any ground truth graph. For the rest of the possible predictions of a pair of nodes (C, A) and (C, B) in any ground truth graph, the error probability for (A, B) remains ϵ (see Lemma B.2). Thus the third column shows the probability of prediction of structure $A \leftarrow C \rightarrow B$ for a particular true graph and the fourth column shows the probability of making an error in predicting the third causal relationship i.e between (A, B) given the first and second pair (C, A) and $((C, B))$ is already predicted. Similarly, the fifth and sixth columns show the same thing for the predicted structure $A \rightarrow C \rightarrow B$ for each of the ground truth graphs. The partial-graph number 4, 7, 8 is not depicted in the table but the entries for 4th graph is the same as 2nd, 7th is the same as 3rd and 8th is same as 6th due to symmetry in the partial-structure. The value of $\epsilon' = \frac{\epsilon}{2-\epsilon}$ in 4th and 6th column is given by renormalized probability Eq. 2 in Lemma B.2.

C ALGORITHMS FOR INTEGRATING CAUSAL ORDER IN EXISTING DISCOVERY METHODS

In continuation to the discussion in Sec 3.2, the algorithms for integrating causal order into existing constraint-based and score-based discovery methods are summarized in Algorithms 1 and 2 respectively.

1026
1027
1028
1029
1030
1031
1032
1033
1034
1035
1036
1037
1038
1039
1040
1041
1042
1043
1044
1045
1046
1047
1048
1049
1050
1051
1052
1053
1054
1055
1056
1057
1058
1059
1060
1061
1062
1063
1064
1065
1066
1067
1068
1069
1070
1071
1072
1073
1074
1075
1076
1077
1078
1079

Dataset	PC	SCORE	ICA LINGAM	Direct LINGAM	NOTEARS	CaMML	Ours (PC+LLM)	Ours (CaMML+LLM)	Ours (PC+Human)	Ours (CaMML+Human)
N = 250	Earthquake	0.16±0.28	4.00±0.00	1.00±0.00	1.00±0.00	1.00±0.00	2.00±0.00	0.00±0.00	0.00±0.00	1.00±0.00
	Cancer	0.00±0.00	3.00±0.00	2.00±0.00	2.00±0.00	2.00±0.00	2.00±0.00	0.00±0.00	0.00±0.00	0.00±0.00
	Survey	0.50±0.00	4.00±0.00	2.00±0.00	4.00±0.00	4.00±0.00	3.33±0.94	0.00±0.00	3.33±0.94	0.00±0.00
	Asia	2.00±0.59	7.00±0.00	3.33±0.47	1.00±0.00	3.00±0.00	1.85±0.58	1.00±0.00	0.97±0.62	N/A
	Asia-M	1.50±0.00	6.00±0.00	1.00±0.00	3.00±0.00	3.00±0.00	1.00±0.00	1.71±0.45	1.00±0.00	2.00±0.00
	Child	5.75±0.00	12.0±0.00	14.33±0.47	16.0±0.00	14.0±0.00	3.00±0.00	4.00±0.00	3.53±0.45	N/A
Neuropathic	4.00±0.00	6.00±0.00	13.0±6.16	10.0±0.00	9.00±0.00	10.4±1.95	3.00±0.00	5.00±0.00	N/A	
N = 500	Earthquake	0.75±0.25	4.0±0.0	1.0±0.0	1.0±0.0	1.0±0.0	0.00±0.00	0.00±0.00	0.00±0.00	0.00±0.00
	Cancer	0.16±0.28	3.00±0.00	3.40±0.48	3.00±0.00	2.00±0.00	1.00±0.00	0.33±0.57	1.00±0.00	0.00±0.00
	Survey	1.25±0.00	4.00±0.00	6.00±0.0	6.00±0.00	3.40±0.48	3.39±0.08	1.00±0.00	3.33±0.94	1.00±0.00
	Asia	3.06±0.00	5.00±0.00	5.60±0.48	7.00±0.00	3.20±0.39	3.81±0.39	1.00±0.00	0.97±0.62	N/A
	Asia-M	2.00±0.00	6.00±0.00	7.60±0.48	5.00±0.00	3.80±0.39	2.00±0.00	1.00±0.00	0.17±0.45	1.33±0.57
	Child	8.09±0.00	6.20±1.32	12.2±0.74	10.6±1.35	15.4±0.48	2.00±0.00	5.00±1.73	2.00±0.00	3.00±0.00
Neuropathic	7.50±0.00	6.00±0.00	9.00±1.41	13.0±0.00	11.0±0.00	5.32±0.57	8.00±0.00	7.49±0.64	N/A	
N = 5000	Earthquake	0.50±0.86	4.00±0.00	2.80±0.39	3.00±0.00	1.00±0.00	0.80±0.97	0.00±0.00	0.00±0.00	0.00±0.00
	Cancer	1.33±0.57	3.00±0.00	3.00±0.00	3.00±0.00	2.00±0.00	2.00±0.00	1.33±0.57	0.00±0.00	0.00±0.00
	Survey	2.00±0.00	4.00±0.00	5.00±0.00	5.00±0.00	3.00±0.00	3.33±0.69	2.00±0.00	2.60±0.00	2.00±0.00
	Asia	1.00±0.00	4.00±0.00	6.60±0.79	4.40±1.35	3.40±0.48	1.75±0.43	0.00±0.00	0.97±0.62	N/A
	Asia-M	2.00±0.00	4.00±0.00	7.60±0.48	4.60±0.48	3.20±0.39	1.68±0.46	2.00±0.00	0.00±0.00	2.00±0.00
	Child	8.25±0.00	3.00±0.00	12.6±0.79	10.8±1.72	14.2±0.40	3.00±0.00	7.00±0.00	3.00±0.00	N/A
Neuropathic	8.62±0.00	6.00±0.00	9.33±0.94	10.0±0.00	10.0±0.00	4.20±0.96	9.00±0.00	1.23±0.42	N/A	
N = 10000	Earthquake	0.00±0.00	4.00±0.00	3.00±0.00	3.00±0.00	1.00±0.00	0.40±0.48	0.00±0.00	0.00±0.00	0.00±0.00
	Cancer	2.00±0.00	3.00±0.00	3.00±0.00	3.00±0.00	2.00±0.00	0.60±0.80	2.00±0.00	0.00±0.00	2.00±0.00
	Survey	2.00±0.00	4.00±0.00	5.00±0.00	5.00±0.00	3.00±0.00	3.60±1.35	2.00±0.00	1.83±0.00	2.00±0.00
	Asia	1.5±0.00	4.00±0.00	6.00±0.00	4.40±1.35	3.00±0.00	1.40±0.48	0.00±0.00	0.34±0.47	N/A
	Asia-M	1.00±0.00	4.00±0.00	8.00±0.00	4.80±0.39	3.00±0.00	2.00±0.00	0.00±0.00	0.00±0.00	3.00±0.00
	Child	6.00±3.04	3.00±0.00	12.2±1.46	11.6±0.48	14.4±0.48	2.80±0.84	5.00±2.64	1.00±0.00	N/A
Neuropathic	10.00±0.00	6.00±0.00	1.00±0.00	10.0±0.00	10.0±0.00	3.00±0.00	10.00±0.00	1.00±0.00	N/A	

Table A3: Comparison with causal discovery methods, showing mean and std dev of D_{top} over 3 runs. (For the Neuropathic subgraph (1k samples), PC Algorithm returns cyclic graphs in the MEC). Human experiments not conducted for Neuropathic, Child (due to feasibility issues) and Asia; hence rows marked as N/A.

Algorithm 1 Integrating $\hat{\pi}$ in constraint-based methods

- 1: **Input:** Noisy expert topological ordering $\hat{\pi}$, Expert \mathcal{E} , CPDAG $\hat{\mathcal{G}}$
- 2: **Output:** Estimated topological order $\hat{\pi}_{final}$ of $\{X_1, \dots, X_n\}$.
- 3: **for** $(i - j) \in \text{undirected-edges}(\hat{\mathcal{G}})$ **do**
- 4: If both nodes i and j are in $\hat{\pi}$ and if $\hat{\pi}_i < \hat{\pi}_j$, orient $(i - j)$ as $(i \rightarrow j)$ in $\hat{\mathcal{G}}$.
- 5: Otherwise, use expert \mathcal{E} to orient the edge.
- 6: **end for**
- 7: $\hat{\pi}_{final} = \text{topological ordering of } \hat{\mathcal{G}}$
- 8: **return** $\hat{\pi}_{final}$

Algorithm 2 Integrating $\hat{\pi}$ in score-based methods

- 1: **Input:** Dataset \mathcal{D} , Variables $\{X_1, \dots, X_n\}$, Expert \mathcal{E} , Score-based method \mathcal{S} , *Prior* probability p .
- 2: **Output:** Estimated topological order $\hat{\pi}_{final}$ of $\{X_1, \dots, X_n\}$.
- 3: $\hat{\mathcal{G}} = \mathcal{E}(X_1, \dots, X_n)$
- 4: $L = \text{level order of } \hat{\mathcal{G}}$
- 5: **for** cycle $C \in \hat{\mathcal{G}}$ **do**
- 6: **for** node $\in C$ **do**
- 7: $L(\text{node}) = \min(\text{level}(c) \forall c \in C)$
- 8: **end for**
- 9: **end for**
- 10: $\hat{\mathcal{G}} = \mathcal{S}(\mathcal{D}, L, p)$ //L is provided as prior
- 11: $\hat{\pi}_{final} = \text{topological ordering of } \hat{\mathcal{G}}$
- 12: **return** $\hat{\pi}_{final}$

D ADDITIONAL RESULTS

D.1 STUDY ON DOWNSTREAM TASKS: CAUSAL DISCOVERY

In continuation to the results presented in Sec 5 of the main paper, we present the performance on the causal discovery task across all sample sizes in Table A3. Evidently, as stated in the main paper, the results show that using expert-provided causal order improves D_{top} across our experiments consistently. CaMML+Human/LLM yields benefits even at higher sample sizes. At a sample size of 10000, CaMML’s D_{top} for Child and Asia surpasses CaMML+LLM by three and fourfold respectively. In specific datasets like *Survey* where the variables are better understood by humans, incorporating human priors to CaMML leads to consistently zero D_{top} , outperforming LLM output.

D.2 D_{top} VS SHD: BETTER MEASURE OF EFFECT ESTIMATION ERROR

As discussed in Sec 3.2 of the main paper, we show herein that D_{top} has a strong correlation with effect estimation error and hence is a valid metric for effect inference.

1080
1081
1082
1083
1084
1085
1086
1087

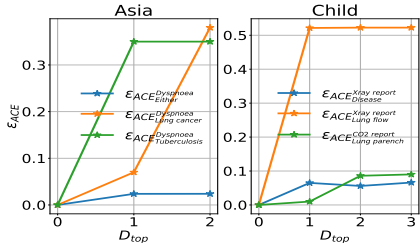


Figure A2: D_{top} vs. ϵ_{ACE} . ϵ_{ACE} increases as D_{top} increases, aligning with theoretical observations.

1088
1089
1090
1091
1092
1093
1094
1095
1096
1097
1098
1099
1100
1101
1102
1103
1104
1105
1106
1107
1108
1109

Cancer			
$D_{top} = 0$		$SHD = 2$	
SHD	ϵ_{ACE}	D_{top}	ϵ_{ACE}
0	0.00	0	0.00
2	0.00	1	0.25
4	0.00	2	0.50

Asia			
$D_{top} = 0$		$SHD = 3$	
SHD	ϵ_{ACE}	D_{top}	ϵ_{ACE}
0	0.00	1	0.14
6	0.00	2	0.22
10	0.00	3	0.57

Survey			
$D_{top} = 0$		$SHD = 2$	
SHD	ϵ_{ACE}	D_{top}	ϵ_{ACE}
0	0.00	0	0.00
2	0.00	1	0.25
4	0.03	2	0.50

Table A4: ϵ_{ACE} vs SHD given D_{top} (& D_{top} given SHD)

1110
1111
1112
1113
1114
1115

D.3 LLMs USED IN POST PROCESSING FOR GRAPH DISCOVERY

We conducted some experiments where we utilised discovery algorithms like PC for creating skeletons of the graph and employed LLMs for orienting the undirected edges. The idea was to utilise LLMs ability to correctly estimate the causal direction while leveraging PC algorithm’s ability to give a skeleton which could be oriented in a post processing setup. We saw that LLM ended up giving improved results as compared to PC alone.

1123
1124
1125

D.4 TRIPLET VS PAIRWISE QUERY STRATEGIES

1127
1128
1129
1130
1131
1132
1133

In continuation to the discussion in Sec 5 of the main paper, we include Tables A5 for more details. The pairwise strategy also shows flaws when LLMs are used as noisy experts. In many cases, pairwise querying yields cycles due to which D_{top} cannot be computed. In particular, for the Child dataset with 20 nodes, pairwise querying of LLMs yields an extremely high number of cycles (see Table A5). LLM output tends to overconnect, resulting in high SHD. Overall, among the prompting strategies, the chain of thought prompt performs the best: it has the lowest number of cycles for Child and Neuropathic datasets. This indicates that in-context examples and chain-of-thought reasoning help to increase the accuracy of causal order output, but other contextual cues do not matter.

1134
1135
1136
1137
1138
1139
1140
1141
1142
1143
1144
1145
1146
1147
1148
1149
1150
1151
1152
1153
1154
1155
1156
1157
1158
1159
1160
1161
1162
1163
1164
1165
1166
1167
1168
1169
1170
1171
1172
1173
1174
1175
1176
1177
1178
1179
1180
1181
1182
1183
1184
1185
1186
1187

Dataset	D _{top}	SHD	IN/TN	Cycles
Base Prompt				
Earthquake	0	7	0/5	0
Cancer	0	6	0/5	0
Survey	3	12	0/6	0
Asia	-	21	0/8	1
Asia-M	-	15	0/7	7
Child	-	177	0/20	>>3k
Neuropathic	-	212	0/22	>>5k
All Directed Edges				
Earthquake	1	9	0/5	0
Cancer	1	7	0/5	0
Survey	2	11	0/6	0
Asia	-	21	0/8	6
Asia-M	0	13	0/7	0
Child	-	139	0/20	>>300
Neuropathic	-	194	0/22	>>1k
One Hop Iteration				
Earthquake	0	8	0/5	0
Cancer	0	6	0/5	0
Survey	3	12	0/6	0
Asia	-	21	0/8	1
Asia-M	0	14	0/7	0
Child	-	167	0/20	>>400
Neuropathic	-	204	0/22	>>4k

Table A5: Comparison of various querying strategies for only LLM-based setups, providing different contextual cues in each setup about the graph. IN: Isolated Nodes, TN:Total Nodes.

Dataset	D _{top}	SHD	IN/TN	Cycles
Chain of Thought				
Earthquake	0	4	0/5	0
Survey	1	9	2/6	0
Asia	-	18	0/8	1
Asia-M	-	13	0/7	1
Child	-	138	0/20	>>500
Neuropathic	-	64	0/22	5
Triplet Query				
Earthquake	0	4	0/5	0
Cancer	1	6	0/5	0
Survey	0	9	0/6	0
Asia	1	14	0/8	0
Asia-M	1	11	0/7	0
Child	-	138	0/20	391
Child (+ Cycle Remover)	1	28	10/20	0
Neuropathic	-	151	0/22	772
Neuropathic(+ Cycle remover)	3	24	13/20	0

Table A6: Triplet query output using variable names with their descriptions (Cancer not included since CoT prompt has examples from this graph). IN: Isolated Nodes, TN:Total Nodes. Since calculating total number of cycles in a DAG is computationally challenging (NP Hard), we find a lower bound of cycles present in each graph based on total k length cycles in each setting, where k=5. If k is scaled up, the number of such unique cycles in the LLM output will also scale significantly. Lower bound helps us make a comparison with number of cycles in outputs like in Triplet strategy, where numbers are comparatively smaller and can be calculated easily.

1188
1189
1190
1191
1192
1193
1194
1195
1196
1197

Dataset	SHD	D_{top}	Cycles	IN/TN
Base Prompt				
Asia	18	1	0	0
Child	148	-	>>10k	0
Earthquake	4	0	0	0
Survey	7	-	1	0
Neuropathic	178	-	>>10k	0
Covid	33	-	15	0
Alzheimers	30	-	1	0

Table A7: Final result of using performing base pairwise querying strategy with GPT-4. These results show how using a superior model in pairwise querying does not lead to complete removal of cycles, further highlighting the impact of triplet strategy.

1201
1202
1203
1204
1205
1206
1207
1208
1209
1210
1211
1212
1213
1214
1215

Dataset	Metric	Pairwise (Base)	Pairwise (CoT)	Triplet
Using Phi-3				
Asia	D_{top}	-	4	0
	SHD	17	11	13
	Cycles	1	0	0
	IN/TN	1/8	0/8	1/8
Alzheimers	D_{top}	-	-	7
	SHD	28	28	25
	Cycles	11	11	0
	IN/TN	0/11	0/11	0/11
Child	D_{top}	-	-	17
	SHD	142	80	69
	Cycles	>>10k	59	0
	IN/TN	0/20	0/20	0/20

1216
1217
1218
1219
1220
1221
1222
1223
1224
1225
1226
1227

Using Llama3				
Asia	D_{top}	-	-	2
	SHD	22	23	17
	Cycles	71	20	0
	IN/TN	0/8	0/8	0/8
Alzheimers	D_{top}	-	-	5
	SHD	41	29	24
	Cycles	1144	7	0
	IN/TN	1/11	0/11	1/11
Child	D_{top}	-	-	12
	SHD	167	151	129
	Cycles	>>10k	71	0
	IN/TN	0/20	0/20	0/20

Table A8: (Top) Results using Phi-3 (Bottom) Performance of triplet method using Llama3 (8b) models vs CoT pairwise vs base pairwise query strategy on multiple benchmark datasets across diff metrics: D_{top} , SHD, (Num of) Cycles, IN (Isolated Nodes), TN (Total Nodes). When num of cycles>0, $\hat{\pi}$ cannot be computed, hence D_{top} is given by '-'. Triplet consistently outperforms the pairwise (base as well as CoT) strategy across metrics & datasets, especially by significant amounts on larger graphs like *Child*.

1234
1235
1236
1237
1238
1239
1240
1241

Finally, the triplet prompt provides the most accurate causal order. For small-scale graphs, it produces no cycles and consistently produces minimal D_{top} (ranging from 0 to 1) while also producing no isolated nodes. Even for medium-size graphs like Child and Neuropathic, the LLM output includes significantly fewer cycles than the pairwise strategy, which were removed leading to a significant and accurate causal order used further as prior. That said, we do see that isolated nodes in the output increase after cycles are removed for medium graphs (all graphs are connected, so outputting an isolated node is an error). Considering LLMs as virtual experts, this indicates that there are some nodes on which the LLM expert cannot determine the causal order. This is still a better tradeoff than providing the wrong causal order, which can confuse downstream algorithms. Overall, we conclude that the triplet query strategy provides the most robust causal order predictions. Additional results

Graphs	Dtop	SHD	Cycles	Isolated Nodes	LLM Calls	Number of Nodes	Complexity
Quadruplet							
Asia	1	6	0	0	70	8	$O(n^3)$
Covid	1	19	0	0	330	11	$O(n^3)$
Alzheimers	5	14	0	0	330	11	$O(n^3)$
Triplet							
Asia	1	14	0	0	286	8	$O(n^4)$
Covid	0	30	0	0	165	11	$O(n^4)$
Alzheimers	4	28	0	0	165	11	$O(n^4)$

Table A9: Analyzing the performance differences between using triplets and quadruplets, we found no significant difference in the quality of the final graph output. However, the number of LLM API calls more than doubles when shifting from triplets to quadruplets, leading to a substantial increase in cost.

Graph	Sample size	Before LLM prior	After LLM Prior
Child	250	18	16
	500	16	15
	1000	14	13
	5000	13.5	12
	10000	9.66	6
Earthquake	250	3.83	3
	500	3.6	3
	1000	3.6	3
	5000	1.16	0.66
	10000	0	0
Cancer	250	1	0
	500	3.83	3.83
	1000	2.6	2.6
	5000	2.3	2.3
	10000	2	2
Asia	250	7.5	7
	500	6	5
	1000	7	7
	5000	2	1
	10000	2	1
Asia-M	250	4.5	4
	500	4	4
	1000	5.5	5
	5000	4	4
	10000	4	4
Neuropathic	250	27	26
	500	31	29
	1000	41	40
	5000	55	53

Table A10: Comparison of SHD Values Before and After Incorporating LLM Priors Using the PC Algorithm Across Various Graphs

showing the error introduced by the LLM with respect to a ground truth order are shown in two different settings in Tables A13 and A14.

1296
1297
1298
1299
1300
1301
1302
1303

Dataset	Samples	LLM	Ground Truth	PC (Average over MEC)
Asia	250	1.00±0.00	0.00±0.00	2.00±0.00
	1000	3.00±0.00	2.00±0.00	3.00±0.00
	10000	3.00±0.00	3.00±0.00	3.00±0.00
Child	250	5.00±0.00	5.00±0.00	6.50±0.00
	1000	6.00±0.00	6.00±0.00	8.43±0.00
	10000	9.00±0.00	9.00±0.00	9.75±0.00

Table A13: Comparing D_{top} of final graph using LLM order vs Ground truth order as prior to PC algorithm for Child and Asia graph, averaged over 4 runs

1304
1305
1306
1307
1308
1309
1310
1311
1312

Dataset	Samples	$\epsilon_{ATE}(S_1)$	$\epsilon_{ATE}(S_2)$	$\epsilon_{ATE}(S_3)$	Δ_{12}	Δ_{13}
Asia	250	0.70±0.40	0.70±0.39	0.69±0.39	0.00±0.00	0.00±0.00
	500	0.64±0.39	0.64±0.39	0.64±0.38	0.00±0.00	0.00±0.00
	1000	0.59±0.32	0.59±0.32	0.59±0.32	0.00±0.00	0.00±0.00
	5000	0.59±0.30	0.59±0.30	0.59±0.29	0.00±0.00	0.00±0.00
	10000	0.49±0.00	0.49±0.00	0.49±0.00	0.00±0.00	0.00±0.00

Table A14: Results on Asia dataset. Here we test the difference in the estimated causal effect of *lung* on *dyspnoea* when the causal effect is estimated using the backdoor set $S_1 = \{smoke\}$ vs. the causal effect estimated when all variables in two topological orders as backdoor sets: $S_2 = \{asia, smoke\}$, $S_3 = \{asia, tub, smoke\}$. Δ_{12}, Δ_{13} refers to the absolute difference between the pairs $\epsilon_{ATE}(S_1), \epsilon_{ATE}(S_2)$ and $\epsilon_{ATE}(S_1), \epsilon_{ATE}(S_3)$ respectively. From the last two columns, we observe that using the variables that come before the treatment node in a topological order as a backdoor set does not result in the deviation of causal effects from the ground truth effects.

1313
1314
1315
1316
1317
1318
1319
1320
1321
1322
1323
1324
1325
1326
1327
1328

Context	1000 samples			
	Base prompt	Past iteration orientations	Markov Blanket	PC (Avg. over MEC)
D_{top}	8.0	5.3	6.6	9.61
SHD	14.33	12.66	14.0	17.0
Context	10000 samples			
	Base prompt	Past iteration orientations	Markov Blanket	PC (Avg. over MEC)
D_{top}	6.33	9.66	6.0	7.67
SHD	9.0	13.33	8.33	12.0

Table A11: PC + LLM results where LLM is used to orient the undirected edges of the skeleton PC returns over different data sample sizes. We show how LLMs can be used in a post processing setup for edge orientation besides having the capability of acting as a strong prior for different discovery algorithms.

1329
1330
1331
1332
1333
1334

E QUERY STRATEGIES: MORE DETAILS AND EXAMPLES

As stated in Sec. D.4, we follow earlier efforts in studying pairwise query strategies in our experiments. Beyond the basic query strategy, we also study its augmentation with additional contextual information. In summary, we study four types of pairwise queries, which we describe below.

1337
1338
1339
1340
1341
1342
1343
1344
1345
1346
1347
1348
1349

- **Basic prompt.** This is the simplest technique. We directly ask the expert to find the causal direction between a given pair of variables (Kiciman et al., 2023).
- **Chain-of-Thought (+ In-context Learning).** Based on encouraging results of providing in-context examples in prompts for various LLM tasks (Brown et al., 2020), we include 3 examples of the ordering task that we expect the expert to perform on. Effectively, we provide example node pairs with their correct causal ordering before asking the question about the given nodes. Each example answer also contains an explanation of the answer, generated using a high-cost expert (GPT-4, in our experiments). Adding the explanation provides the expert with additional reasoning information when deciding the causal order (Wei et al., 2022). To avoid overfitting, we select node pairs from graphs that are not evaluated in our study, as additional input. Node pairs with and without direct edges were equally chosen for this purpose. Examples of an expert’s (LLM’s in this case) answers (and their explanations) using this query strategy are shown in tables below.
- **Iterative Context.** Here, we provide previously oriented pairs as context in the prompt. Since the expert has access to its previous decisions, we expect that it may avoid creating cycles through its predictions.
- **One hop iterative Context.** Providing previously oriented pairs may become prohibitive for large graphs. Here we provide the information of connections with neighbouring nodes of the node pair being inspected as additional context in the query.

Dataset	Number of Nodes	Number of Edges	Description (used as a context)
Asia	8	8	Model the possible respiratory problems someone can have who has recently visited Asia and is experiencing shortness of breath
Cancer	5	4	Model the relation between various variables responsible for causing Cancer and its possible outcomes
Earthquake	5	5	Model factors influencing the probability of a burglary
Survey	6	6	Model a hypothetical survey whose aim is to investigate the usage patterns of different means of transport
Child	20	25	Model congenital heart disease in babies
Neuropathic Pain Diagnosis (subgraph)	22	25	For neuropathic pain diagnosis

Table A15: Overview of datasets used

Cost Estimation Analysis: Pairwise vs. Triplet for LLMs

Triplet method ensures scalability by optimizing most calls to a cheaper and smaller model (like GPT-3.5-Turbo) while improving performance. The triplet pipeline boosts accuracy through multiple context switches (varying the third node) for better pairwise orientation. Strategic use of GPT-4 for conflict resolution enhances effectiveness and controls costs. For a 100-node graph, pairwise orientation using GPT-4 costs an estimated \$574, while our triplet strategy, leveraging both GPT-4 and GPT-3.5-Turbo, reduces costs to \$55. Although our triplet method involves more calls, it optimally uses GPT-4 for error correction, significantly improving performance while keeping costs low.

F CAUSAL GRAPHS USED IN EXPERIMENTS

Figures A3-A7 show the causal graphs and details we considered from BNLearn repository (Scutari & Denis, 2014).

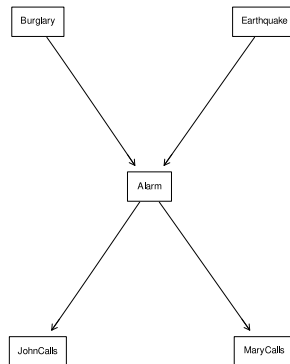


Figure A3: Earthquake Bayesian network. Abbreviations/Descriptions: Burglary: *burglar entering*, Earthquake: *earthquake hitting*, Alarm: *home alarm going off in a house*, JohnCalls: *first neighbor to call to inform the alarm sound*, MaryCalls: *second neighbor to call to inform the alarm sound*.

1404
 1405
 1406
 1407
 1408
 1409
 1410
 1411
 1412
 1413
 1414
 1415
 1416
 1417
 1418
 1419
 1420
 1421
 1422
 1423
 1424
 1425
 1426
 1427
 1428
 1429
 1430
 1431
 1432
 1433
 1434
 1435
 1436
 1437
 1438
 1439
 1440
 1441
 1442
 1443
 1444
 1445
 1446
 1447
 1448
 1449
 1450
 1451
 1452
 1453
 1454
 1455
 1456
 1457

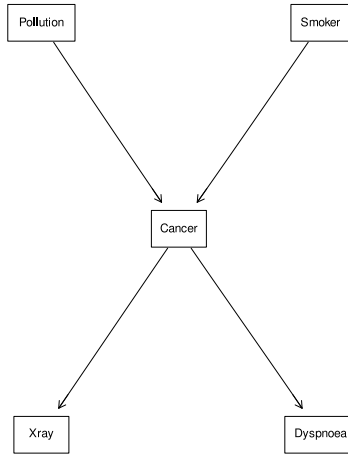


Figure A4: Cancer Bayesian network. Abbreviations/Descriptions: Pollution: *exposure to pollutants*, Smoker: *smoking habit*, Cancer: *Cancer*, Dyspnoea: *Dyspnoea*, Xray: *getting positive xray result*.

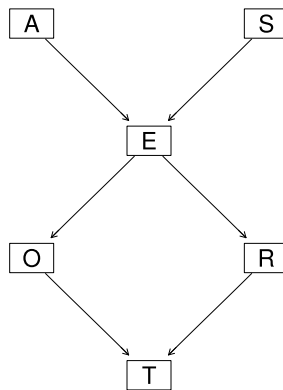


Figure A5: Survey Bayesian network. Abbreviations: A=Age/Age of people using transport, S=Sex/male or female, E=Education/up to high school or university degree, O=Occupation/employee or self-employed, R=Residence/the size of the city the individual lives in, recorded as either small or big, T=Travel/the means of transport favoured by the individual.

1458
1459
1460
1461
1462
1463
1464
1465
1466
1467
1468
1469
1470
1471
1472
1473
1474
1475
1476
1477
1478
1479
1480
1481
1482
1483
1484
1485
1486
1487
1488
1489
1490
1491
1492
1493
1494
1495
1496
1497
1498
1499
1500
1501
1502
1503
1504
1505
1506
1507
1508
1509
1510
1511

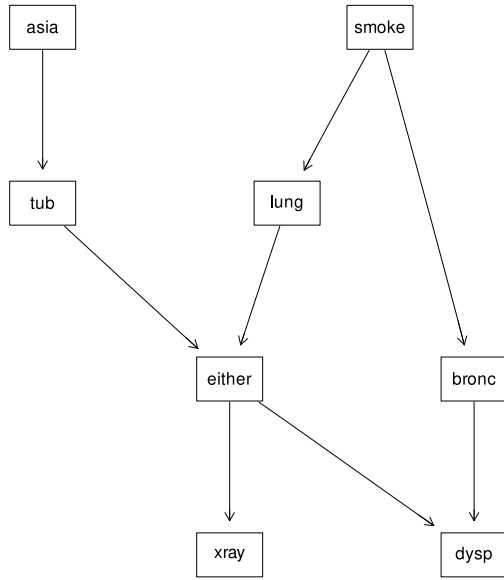


Figure A6: Asia Bayesian network. Abbreviations/Descriptions: asia=visit to Asia/visiting Asian countries with high exposure to pollutants, smoke=smoking habit, tub=tuberculosis, lung=lung cancer, either=either tuberculosis or lung cancer, bronc=bronchitis, dysp=dyspnoea, xray=getting positive xray result.

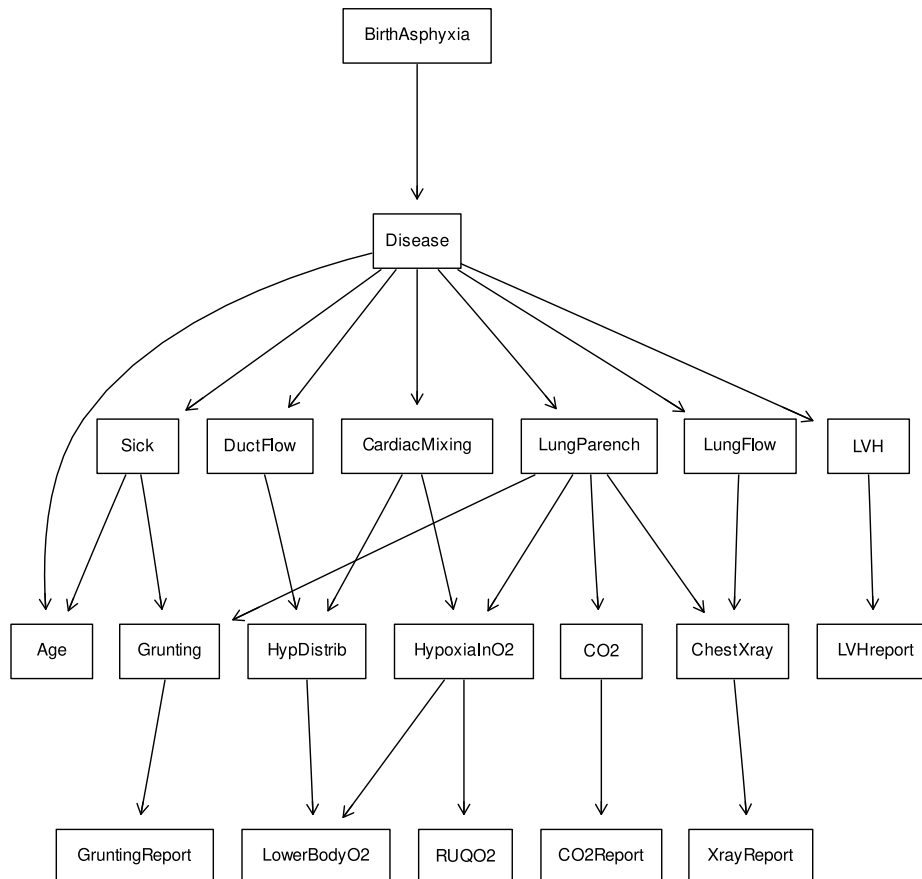


Figure A7: Child Bayesian network. Abbreviations: BirthAsphyxia: *Lack of oxygen to the blood during the infant's birth*, HypDistrib: *Low oxygen areas equally distributed around the body*, HypoxiaInO2: *Hypoxia when breathing oxygen*, CO2: *Level of carbon dioxide in the body*, ChestXray: *Having a chest x-ray*, Grunting: *Grunting in infants*, LVHreport: *Report of having left ventricular hypertrophy*, LowerBodyO2: *Level of oxygen in the lower body*, RUQO2: *Level of oxygen in the right upper quadricer muscle*, CO2Report: *A document reporting high levels of CO2 levels in blood*, XrayReport: *Report of having a chest x-ray*, Disease: *Presence of an illness*, GruntingReport: *Report of infant grunting*, Age: *Age of infant at disease presentation*, LVH: *Thickening of the left ventricle*, DuctFlow: *Blood flow across the ductus arteriosus*, CardiacMixing: *Mixing of oxygenated and deoxygenated blood*, LungParench: *The state of the blood vessels in the lungs*, LungFlow: *Low blood flow in the lungs*, Sick: *Presence of an illness*

1566
 1567
 1568
 1569
 1570
 1571
 1572
 1573
 1574
 1575
 1576
 1577
 1578
 1579
 1580
 1581
 1582
 1583
 1584
 1585
 1586
 1587
 1588
 1589
 1590
 1591
 1592
 1593
 1594
 1595
 1596
 1597
 1598
 1599
 1600
 1601
 1602
 1603
 1604
 1605
 1606
 1607
 1608
 1609
 1610
 1611
 1612
 1613
 1614
 1615
 1616
 1617
 1618
 1619

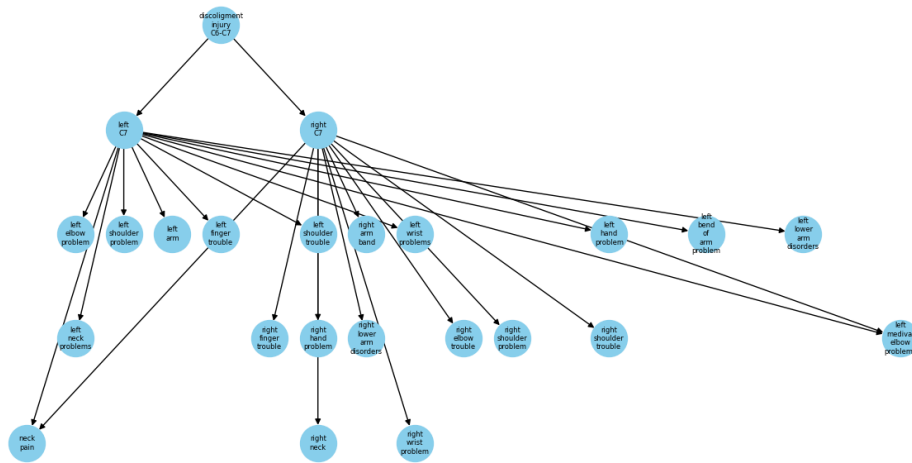


Figure A8: For Neuropathic dataset, we consider a sub-graph induced by one of the root nodes, containing the following 22 nodes and corresponding edges taken from <https://observablehq.com/@turuibo/the-complete-causal-graph-of-neuropathic-pain-diagnosis>: 'right C7', 'right elbow trouble', 'left shoulder trouble', 'left bend of arm problem', 'right shoulder trouble', 'right hand problem', 'left medial elbow problems', 'right finger trouble', 'left neck problems', 'left wrist problems', 'left shoulder problem', 'right neck', 'right wrist problem', 'right shoulder problem', 'discoligment injury C6 C7', 'left hand problem', 'left C7', 'right arm band', 'left lower arm disorders', 'neck pain', 'left finger trouble', 'left arm'. We did not use descriptions for the nodes of Neuropathic graph.

1620
 1621
 1622
 1623
 1624
 1625
 1626
 1627
 1628
 1629
 1630
 1631
 1632
 1633
 1634
 1635
 1636
 1637
 1638
 1639
 1640
 1641
 1642
 1643
 1644
 1645
 1646
 1647
 1648
 1649
 1650
 1651
 1652
 1653
 1654
 1655
 1656
 1657
 1658
 1659
 1660
 1661
 1662
 1663
 1664
 1665
 1666
 1667
 1668
 1669
 1670
 1671
 1672
 1673

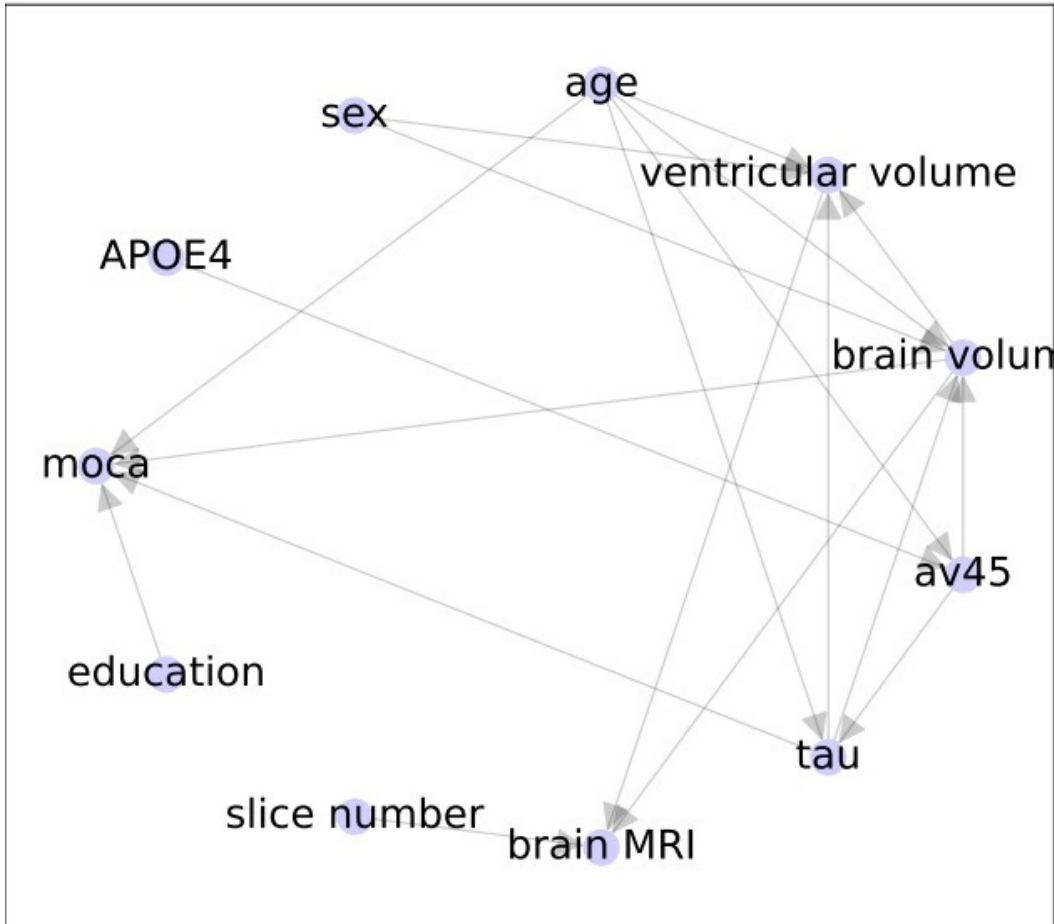


Figure A9: The **Alzheimer's dataset** is a Bayesian Network developed by Abdulaal, Ahmed, et al. in collaboration with five domain experts, as detailed in their paper "Causal Modelling Agents: Causal Graph Discovery through Synergising Metadata-and Data-driven Reasoning" (ICLR 2024). The dataset includes the following variables: **age**, which represents the age of the patient; **sex**, indicating the biological sex of the patient; **APOE4**, which measures the expression level of the APOE4 gene; **education**, reflecting the patient's educational attainment in years; **av45**, measuring the beta amyloid protein level using Florbetapir F 18; **tau**, indicating phosphorylated-tau deposition; **brain volume**, representing the total brain matter volume of the patient; **Ventricular Volume**, indicating the total ventricular volume of the patient; and **moca**, which is the Montreal Cognitive Assessment Score.

1674
1675
1676
1677
1678
1679
1680
1681
1682
1683
1684
1685
1686
1687
1688
1689
1690
1691
1692
1693
1694
1695
1696
1697
1698
1699
1700
1701
1702
1703
1704
1705
1706
1707
1708
1709
1710
1711
1712
1713
1714
1715
1716
1717
1718
1719
1720
1721
1722
1723
1724
1725
1726
1727

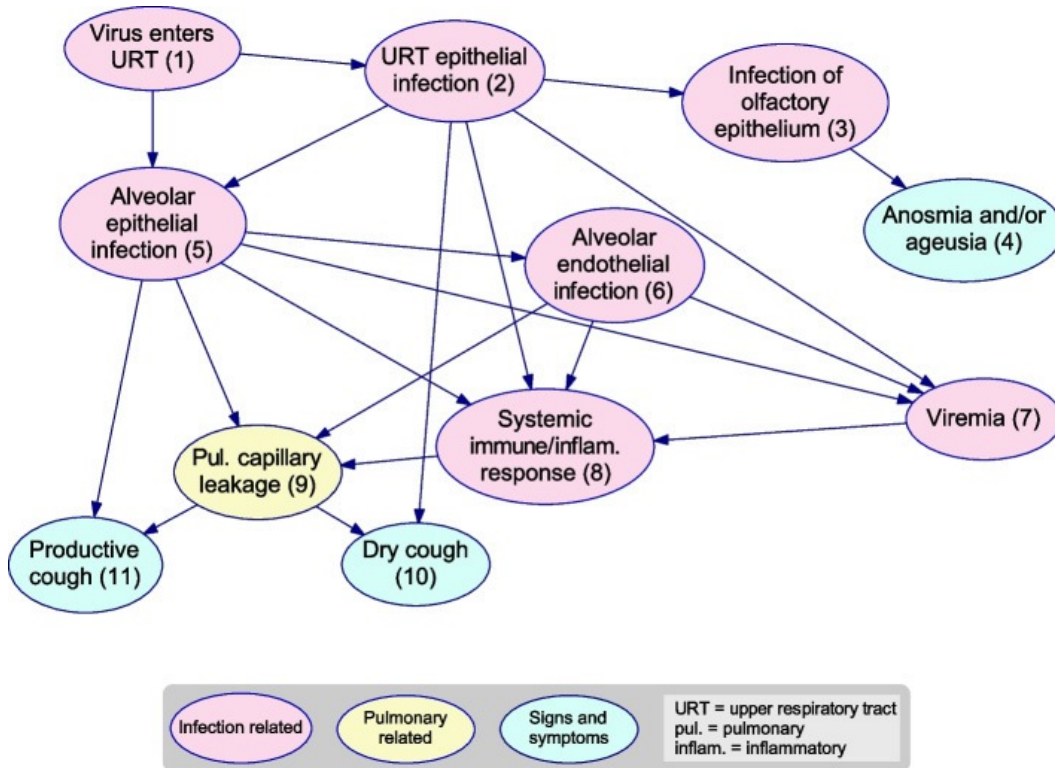


Figure A10: **Respiratory causal DAG** taken from Mascaro S, Wu Y, Woodberry O, et al. Modeling COVID-19 disease processes by remote elicitation of causal Bayesian networks from medical experts. BMC Med Res Methodol. Here, **Virus enters upper respiratory tract (URT)**: SARS-CoV-2 viral particles inhaled and attach to upper respiratory tract mucosal surface. The size of the viral inoculum is dependent on exposure related factors, not included in the current model, **Upper respiratory tract (URT) epithelial infection**: Viral infection of upper respiratory tract epithelial cells +/- signaling an immune response and leading to local inflammation, **Infection of olfactory epithelium**: Viral infection of the olfactory epithelial cells +/- leading to impaired olfaction, **Ageusia and/or anosmia**: Loss of the ability to taste and/or smell, **Alveolar epithelial infection**: Viral infection of the alveolar cells, +/- inducing an immune response which leads to local inflammation. **Alveolar endothelial infection**: Viral infection of the endothelial cells of the capillaries of the terminal airways, +/- inducing an immune response which leads to local inflammation., **Viremi**: Presence of SARS-CoV-2 in blood allowing for systemic dissemination of the virus., **Systemic immune/inflammatory (inflam.) response**: Activation of innate and/or adaptive immune system by the presence of virus at one or more body site/s. Manifest by the release of pro- +/- anti-inflammatory markers in blood by immune-related cells, **Pulmonary capillary leakage**: Leakage of plasma from the pulmonary capillaries into the terminal airways., leakage **Dry cough**: Cough without the production of mucus or phlegm., **Productive cough**: Cough with the production of mucus or phlegm.

1728	Question: For a causal graph used to model relationship of various factors and outcomes related to cancer
1729	with the following nodes: ['Pollution', 'Cancer', 'Smoker', 'Xray', 'Dyspnoea'],
1730	Which cause-and-effect relationship is more likely between nodes 'smoker' and 'cancer'?
1731	
1732	A. changing the state of node 'smoker' causally affects a change in another node 'cancer'.
1733	
1734	B. changing the state of node 'cancer' causally affects a change in another node 'smoker'.
1735	
1736	C. There is no causal relation between the nodes 'cancer' and 'smoker'.
1737	Make sure to first provide a grounded reasoning for your answer and then provide the answer in the
1738	following format: <Answer>A/B/C/</Answer>. It is very important that you output the final Causal graph
1739	within the tags like <Answer>A/B/C/</Answer> otherwise your answer will not be processed.
1740	Answer: The causal effect of "smoker" directing to "cancer" is based on the strong evidence from epidemi-
1741	ological studies linking smoking to an increased risk of developing cancer. Smoking introduces harmful
1742	substances into the respiratory system, leading to cellular damage and mutation, which significantly
1743	raises the likelihood of cancer development in the lungs or respiratory tract, subsequently impacting the
1744	occurrence of respiratory problems like shortness of breath. Therefore answer is <Answer>A/</Answer>
1745	Question: For a causal graph used to model relationship of various factors and outcomes related to cancer
1746	with the following nodes: ['Pollution', 'Cancer', 'Smoker', 'Xray', 'Dyspnoea'], Which cause-and-effect
1747	relationship is more likely between nodes 'xray' and 'dyspnoea'?
1748	
1749	A. changing the state of node 'xray' causally affects a change in another node 'dyspnoea'.
1750	
1751	B. changing the state of node 'dyspnoea' causally affects a change in another node 'xray'.
1752	
1753	C. There is no causal relation between the nodes 'xray' and 'dyspnoea'.
1754	Make sure to first provide a grounded reasoning for your answer and then provide the answer in the
1755	following format: <Answer>A/B/C/</Answer>. It is very important that you output the final Causal graph
1756	within the tags like <Answer>A/B/C/</Answer> otherwise your answer will not be processed.
1757	Answer: Reasoning behind the lack of causal relation between X-ray and dyspnoea is that X-ray and
1758	dyspnoea are both effects of having cancer, but they do not directly cause or affect each other. X-ray is a
1759	diagnostic test that can help detect cancer in the lungs or other organs, while dyspnoea is a symptom of
1760	cancer that involves feeling short of breath. Therefore, X-ray and dyspnoea are not causally related, but
1761	they are both associated with cancer. Therefore answer is <Answer>C/</Answer>
1762	Question: For a causal graph used to model relationship of various factors and outcomes related to cancer
1763	with the following nodes: ['Pollution', 'Cancer', 'Smoker', 'Xray', 'Dyspnoea'], Which cause-and-effect
1764	relationship is more likely between nodes 'xray' and 'cancer'?
1765	
1766	A. changing the state of node 'xray' causally affects a change in another node 'cancer'.
1767	
1768	B. changing the state of node 'cancer' causally affects a change in another node 'xray'.
1769	
1770	C. There is no causal relation between the nodes 'xray' and 'cancer'.
1771	Make sure to first provide a grounded reasoning for your answer and then provide the answer in the
1772	following format: <Answer>A/B/C/</Answer>. It is very important that you output the final Causal graph
1773	within the tags like <Answer>A/B/C/</Answer> otherwise your answer will not be processed.

Table A16: Chain of Thought Prompt

1774
1775
1776
1777
1778
1779
1780
1781

1782
1783
1784
1785
1786
1787
1788
1789
1790
1791
1792
1793
1794
1795
1796
1797
1798
1799
1800
1801
1802
1803
1804
1805
1806
1807
1808
1809
1810
1811
1812
1813
1814
1815
1816
1817
1818
1819
1820
1821
1822
1823
1824
1825
1826
1827
1828
1829
1830
1831
1832
1833
1834
1835

Answer: The causal effect of cancer on X-ray is that X-rays are often used to diagnose or detect cancer in different parts of the body, such as the bones, lungs, breasts, or kidneys¹²³. X-rays use low doses of radiation to create pictures of the inside of the body and show the presence, size, and location of tumors. X-rays can also help monitor the response to treatment or check for signs of recurrence. Therefore, having cancer may increase the likelihood of getting an X-ray as part of the diagnostic process or follow-up care. Therefore answer is `<Answer>B</Answer>`

Question: For a causal graph used to model relationship of various factors and outcomes related to cancer with the following nodes: ['Pollution', 'Cancer', 'Smoker', 'Xray', 'Dyspnoea'], Which cause-and-effect relationship is more likely between nodes 'pollution' and 'cancer'?

- A. changing the state of node 'pollution' causally affects a change in another node 'cancer'.
- B. changing the state of node 'cancer' causally affects a change in another node 'pollution'.
- C. There is no causal relation between the nodes 'pollution' and 'cancer'.

Make sure to first provide a grounded reasoning for your answer and then provide the answer in the following format: `<Answer>A/B/C</Answer>`. It is very important that you output the final Causal graph within the tags like `<Answer>A/B/C</Answer>` otherwise your answer will not be processed.

Answer: The causal effect of pollution on cancer is that air pollution contains carcinogens (cancer-causing substances) that may be absorbed into the body when inhaled and damage the DNA of cells. Another possible reasoning is that particulate matter (tiny dust-like particles) in air pollution may cause physical damage to the cells in the lungs, leading to inflammation and oxidative stress and eventually cell mutations. A third possible reasoning is that air pollution may create an inflamed environment in the lungs that encourages the proliferation of cells with existing cancer-driving mutations. These are some of the hypotheses that researchers have proposed to explain how air pollution may cause cancer, but more studies are needed to confirm them. Therefore answer is `<Answer>A</Answer>`

Question: For a causal graph used to model relationship of various factors and outcomes related to cancer with the following nodes: ['Pollution', 'Cancer', 'Smoker', 'Xray', 'Dyspnoea'], Which cause-and-effect relationship is more likely between nodes 'pollution' and 'smoker'?

- A. changing the state of node 'pollution' causally affects a change in another node 'smoker'.
- B. changing the state of node 'smoker' causally affects a change in another node 'pollution'.
- C. There is no causal relation between the nodes 'pollution' and 'smoker'.

Make sure to first provide a grounded reasoning for your answer and then provide the answer in the following format: `<Answer>A/B/C</Answer>`. It is very important that you output the final Causal graph within the tags like `<Answer>A/B/C</Answer>` otherwise your answer will not be processed.

Answer: Reason behind the lack of causal relation between pollution and smoker is that pollution and smoking are both independent risk factors for respiratory problems, but they do not directly cause or affect each other. Pollution and smoking both contribute to air pollution, which can harm the health of people and the environment. However, pollution is mainly caused by human activities such as burning fossil fuels, deforestation, or industrial processes, while smoking is a personal choice that involves inhaling tobacco smoke. Therefore, pollution and smoker are not causally related, but they are both associated with respiratory problems. Therefore answer is `<Answer>C</Answer>`.

Table A17: Chain of Thought Prompt (continued..)

1836
1837
1838
1839
1840
1841
1842
1843
1844
1845
1846
1847
1848
1849
1850
1851
1852
1853
1854
1855
1856
1857
1858
1859
1860
1861
1862
1863
1864
1865
1866
1867
1868
1869
1870
1871
1872
1873
1874
1875
1876
1877
1878
1879
1880
1881
1882
1883
1884
1885
1886
1887
1888
1889

Question: For a causal graph used for modeling factors causing Coronary Heart Diseases with the following nodes: ['Family Disease', 'Gene', 'Smoking', 'Blood Pressure', 'Coronary Heart Disease', 'Headache'], Which cause-and-effect relationship is more likely between nodes 'Family Disease' and 'Gene'?

- A. changing the state of node 'Family Disease' causally affects a change in another node 'Gene'.
- B. changing the state of node 'Gene' causally affects a change in another node 'Family Disease'.
- C. There is no causal relation between the nodes 'Family Disease' and 'Gene'.

Make sure to first provide a grounded reasoning for your answer and then provide the answer in the following format: $\langle \text{Answer} \rangle A/B/C / \langle \text{Answer} \rangle$. It is very important that you output the final Causal graph within the tags like $\langle \text{Answer} \rangle A/B/C / \langle \text{Answer} \rangle$ otherwise your answer will not be processed.

Answer: Reason behind the causal effect of family disease on gene is that family disease is a term that refers to diseases or health conditions that run in the family, meaning that they are influenced by genetic factors. Gene is a term that refers to the basic unit of heredity that carries information for a specific trait or function. Family disease can affect gene by altering the type or frequency of genes that are inherited by the offspring from their parents. For example, some family diseases are caused by deterministic genes, which are genes that guarantee the development of a disease if they are present in a person's genome. Other family diseases are influenced by risk genes, which are genes that increase the likelihood of developing a disease but do not guarantee it. Therefore, family disease can causally direct to gene by changing the genetic makeup of a person or a population. Therefore answer is $\langle \text{Answer} \rangle A / \langle \text{Answer} \rangle$.

Question: For a causal graph used for modeling factors causing Coronary Heart Diseases with the following nodes: ['Family Disease', 'Gene', 'Smoking', 'Blood Pressure', 'Coronary Heart Disease', 'Headache'], Which cause-and-effect relationship is more likely between nodes 'Coronary Heart Disease' and 'Gene'?

- A. changing the state of node 'Coronary Heart Disease' causally affects a change in another node 'Gene'.
- B. changing the state of node 'Gene' causally affects a change in another node 'Coronary Heart Disease'.
- C. There is no causal relation between the nodes 'Coronary Heart Disease' and 'Gene'.

Make sure to first provide a grounded reasoning for your answer and then provide the answer in the following format: $\langle \text{Answer} \rangle A/B/C / \langle \text{Answer} \rangle$. It is very important that you output the final Causal graph within the tags like $\langle \text{Answer} \rangle A/B/C / \langle \text{Answer} \rangle$ otherwise your answer will not be processed.

Answer: Possible reasoning behind the causal effect of gene on coronary heart disease is that gene is a term that refers to the basic unit of heredity that carries information for a specific trait or function. Gene can affect coronary heart disease by influencing the structure and function of the blood vessels, the metabolism and transport of lipids (fats) in the blood, the inflammation and clotting processes, or the response to environmental factors such as smoking or diet. For example, some genes code for proteins that regulate the cell cycle and growth of the cells that line the arteries, which can affect their susceptibility to damage or plaque formation. Other genes code for proteins that control the synthesis and clearance of cholesterol or other lipids, which can affect their levels and deposition in the arteries. Therefore, gene can causally direct to coronary heart disease by modifying the biological pathways that contribute to the development or progression of the disease. Therefore answer is $\langle \text{Answer} \rangle B / \langle \text{Answer} \rangle$

Table A18: Chain of Thought Prompt (continued..)

1890
1891
1892
1893
1894
1895
1896
1897
1898
1899
1900
1901
1902
1903
1904
1905
1906
1907
1908
1909
1910
1911
1912
1913
1914
1915
1916
1917
1918
1919
1920
1921
1922
1923
1924
1925
1926
1927
1928
1929
1930
1931
1932
1933
1934
1935
1936
1937
1938
1939
1940
1941
1942
1943

Question: For a causal graph used for modeling factors causing Coronary Heart Diseases with the following nodes: ['Family Disease', 'Gene', 'Smoking', 'Blood Pressure', 'Coronary Heart Disease', 'Headache'], Which cause-and-effect relationship is more likely between nodes 'Blood Pressure' and 'Smoking'?

- A. changing the state of node 'Blood Pressure' causally affects a change in another node 'Smoking'.
- B. changing the state of node 'Smoking' causally affects a change in another node 'Blood Pressure'.
- C. There is no causal relation between the nodes 'Blood Pressure' and 'Smoking'.

Make sure to first provide a grounded reasoning for your answer and then provide the answer in the following format: `<Answer>A/B/C</Answer>`. It is very important that you output the final Causal graph within the tags like `<Answer>A/B/C</Answer>` otherwise your answer will not be processed.

Answer: Possible reasoning behind the causal effect of smoking on blood pressure is that smoking is a habit that involves inhaling tobacco smoke, which contains nicotine and other harmful chemicals. Smoking can affect blood pressure by activating the sympathetic nervous system (SNS), which is the part of the nervous system that controls the body's response to stress or danger. When the SNS is activated, it releases hormones such as adrenaline and noradrenaline, which cause the heart to beat faster and harder, and the blood vessels to constrict. This results in a temporary increase in blood pressure, which can last for 15 to 20 minutes after each cigarette. Therefore, smoking can causally direct to blood pressure by stimulating the SNS and increasing the cardiac output and vascular resistance. Therefore answer is `<Answer>B</Answer>`.

Question: For a causal graph used for modeling factors causing Coronary Heart Diseases with the following nodes: ['Family Disease', 'Gene', 'Smoking', 'Blood Pressure', 'Coronary Heart Disease', 'Headache'], Which cause-and-effect relationship is more likely between nodes 'Headache' and 'Smoking'?

- A. changing the state of node 'Headache' causally affects a change in another node 'Smoking'.
- B. changing the state of node 'Smoking' causally affects a change in another node 'Headache'.
- C. There is no causal relation between the nodes 'Headache' and 'Smoking'.

Make sure to first provide a grounded reasoning for your answer and then provide the answer in the following format: `<Answer>A/B/C</Answer>`. It is very important that you output the final Causal graph within the tags like `<Answer>A/B/C</Answer>` otherwise your answer will not be processed.

Answer: One possible reasoning behind the lack of causal relation between headache and smoking is that headache and smoking are both associated with various health conditions, but they do not directly cause or affect each other¹². Headache is a term that refers to pain or discomfort in the head, scalp, or neck, which can have many possible causes, such as stress, dehydration, infection, injury, or medication. Smoking is a habit that involves inhaling tobacco smoke, which contains nicotine and other harmful chemicals, which can increase the risk of diseases such as cancer, heart disease, stroke, and lung disease. Therefore, headache and smoking are not causally related, but they are both linked to different health problems. Therefore the answer is `<Answer>C</Answer>`

Table A19: Chain of Thought Prompt (continued..)

1944

1945

1946

1947

1948

1949

1950

1951

1952

1953

1954

1955

1956

1957

1958

1959

1960

1961

1962

1963

1964

1965

1966

1967

1968

1969

1970

1971

1972

1973

1974

1975

1976

1977

1978

1979

1980

1981

1982

1983

1984

1985

1986

1987

1988

1989

1990

1991

1992

1993

1994

1995

1996

1997

Question: For a causal graph used for modeling factors causing Coronary Heart Diseases with the following nodes: ['Family Disease', 'Gene', 'Smoking', 'Blood Pressure', 'Coronary Heart Disease', 'Headache'], Which cause-and-effect relationship is more likely between nodes 'Headache' and 'Smoking'?

A. changing the state of node 'Headache' causally affects a change in another node 'Smoking'.

B. changing the state of node 'Smoking' causally affects a change in another node 'Headache'.

C. There is no causal relation between the nodes 'Headache' and 'Smoking'.

Make sure to first provide a grounded reasoning for your answer and then provide the answer in the following format: $\langle \text{Answer} \rangle A/B/C / \langle \text{Answer} \rangle$. It is very important that you output the final Causal graph within the tags like $\langle \text{Answer} \rangle A/B/C / \langle \text{Answer} \rangle$ otherwise your answer will not be processed.

Answer: One possible reasoning behind the lack of causal relation between headache and smoking is that headache and smoking are both associated with various health conditions, but they do not directly cause or affect each other. Headache is a term that refers to pain or discomfort in the head, scalp, or neck, which can have many possible causes, such as stress, dehydration, infection, injury, or medication. Smoking is a habit that involves inhaling tobacco smoke, which contains nicotine and other harmful chemicals, which can increase the risk of diseases such as cancer, heart disease, stroke, and lung disease. Therefore, headache and smoking are not causally related, but they are both linked to different health problems. Therefore the answer is $\langle \text{Answer} \rangle C / \langle \text{Answer} \rangle$

Question: For a causal graph used for modeling factors causing Coronary Heart Diseases with the following nodes: ['Family Disease', 'Gene', 'Smoking', 'Blood Pressure', 'Coronary Heart Disease', 'Headache'], Which cause-and-effect relationship is more likely between nodes 'Coronary Heart Disease' and 'Smoking'?

A. changing the state of node 'Smoking' causally affects a change in another node 'Coronary Heart Disease'.

B. changing the state of node 'Coronary Heart Disease' causally affects a change in another node 'Smoking'.

C. There is no causal relation between the nodes 'Coronary Heart Disease' and 'Smoking'.

Make sure to first provide a grounded reasoning for your answer and then provide the answer in the following format: $\langle \text{Answer} \rangle A/B/C / \langle \text{Answer} \rangle$. It is very important that you output the final Causal graph within the tags like $\langle \text{Answer} \rangle A/B/C / \langle \text{Answer} \rangle$ otherwise your answer will not be processed.

Answer: Possible reasoning behind the causal effect of smoking on coronary heart disease is smoking damages the heart and blood vessels by raising triglycerides, lowering HDL, increasing blood clotting, and impairing blood flow to the heart. This can lead to plaque buildup, heart attacks, and death. Therefore answer is $\langle \text{Answer} \rangle A / \langle \text{Answer} \rangle$.

Question: For a causal graph used for context with the following nodes: nodes, Which cause-and-effect relationship is more likely between nodes X and Y?

A. changing the state of node X causally affects a change in another node Y.

B. changing the state of node Y causally affects a change in another node X.

C. There is no causal relation between the nodes X and Y.

Make sure to first provide a grounded reasoning for your answer and then provide the answer in the following format: $\langle \text{Answer} \rangle A/B/C / \langle \text{Answer} \rangle$. It is very important that you output the final Causal graph within the tags like $\langle \text{Answer} \rangle A/B/C / \langle \text{Answer} \rangle$ otherwise your answer will not be processed.

Table A20: Chain of Thought Queries (continued..)

1998
1999
2000
2001
2002
2003
2004
2005
2006
2007
2008
2009
2010
2011
2012
2013
2014
2015
2016
2017
2018
2019
2020
2021
2022
2023
2024
2025
2026
2027
2028
2029
2030
2031
2032
2033
2034
2035
2036
2037
2038
2039
2040
2041
2042
2043
2044
2045
2046
2047
2048
2049
2050
2051

Which cause-and-effect relationship is more likely?

A. changing the state of node which says X causally affects a change in another node which says Y.

B. changing the state of node which says Y causally affects a change in another node which says X.

C. There is no causal relationship between node X and Y.

Make sure to first output a factually grounded reasoning for your answer. X and Y are nodes of a Causal Graph. The causal graph is sparse and acyclic in nature. So option C could be chosen if there is some uncertainty about causal relationship between X and Y.

First give your reasoning and after that please make sure to provide your final answer within the tags `<Answer>A/B/C</Answer>`.

It is very important that you output your final answer between the tags like `<Answer>A/B/C</Answer>` otherwise your response will not be processed.

Table A21: Base Queries

For the nodes X and Y which form an edge in a Causal Graph, you have to identify which cause-and-effect relationship is more likely between the nodes of the edge. This will be used to rearrange the nodes in the edge to create a directed edge which accounts for causal relation from one node to another in the edge.

A. changing the state of node X causally affects a change in another node Y.

B. changing the state of node Y causally affects a change in another node X.

C. There is no causal relation between the nodes X and Y.

You can also take the edges from the skeleton which have been rearranged to create a directed edge to account for causal relationship between the nodes: `directed_edges`.

Make sure to first output a factually grounded reasoning for your answer. First give your reasoning and after that please make sure to provide your final answer within the tags `<Answer>A/B/C</Answer>`.

It is very important that you output your final answer between the tags like `<Answer>A/B/C</Answer>` otherwise your response will not be processed.

Table A22: Iterative orientation Queries

2052
2053
2054
2055
2056
2057
2058
2059
2060
2061
2062
2063
2064
2065
2066
2067
2068
2069
2070
2071
2072
2073
2074
2075
2076
2077
2078
2079
2080
2081
2082
2083
2084
2085
2086
2087
2088
2089
2090
2091
2092
2093
2094
2095
2096
2097
2098
2099
2100
2101
2102
2103
2104
2105

For the following undirected edge in a Causal Graph made of nodes X and Y, you have to identify which cause-and-effect relationship is more likely between the nodes of the edge. This will be used to rearrange the nodes in the edge to create a directed edge which accounts for causal relation from one node to another in the edge.

- A. changing the state of node X causally affects a change in another node Y.
- B. changing the state of node Y causally affects a change in another node X.
- C. There is no causal relation between the nodes X and Y.

You can also take the other directed edges of nodes X: X_edges and Y: Y_edges of the Causal graph as context to redirect the edge to account for causal effect.

Make sure to first output a factually grounded reasoning for your answer. First give your reasoning and after that please make sure to provide your final answer within the tags `<Answer>A/B/C</Answer>`.

It is very important that you output your final answer between the tags like `<Answer>A/B/C</Answer>` otherwise your response will not be processed.

Table A23: Iterative One Hop Queries

*Identify the causal relationships between the given variables and create a directed acyclic graph to **{context}**. Make sure to give a reasoning for your answer and then output the directed graph in the form of a list of tuples, where each tuple is a directed edge. The desired output should be in the following form: [(‘A’, ‘B’), (‘B’, ‘C’)] where first tuple represents a directed edge from Node ‘A’ to Node ‘B’, second tuple represents a directed edge from Node ‘B’ to Node ‘C’ and so on.*

If a node should not form any causal relationship with other nodes, then you can add it as an isolated node of the graph by adding it separately. For example, if ‘C’ should be an isolated node in a graph with nodes ‘A’, ‘B’, ‘C’, then the final DAG representation should be like [(‘A’, ‘B’), (‘C’)].

Use the description about the node provided with the nodes in brackets to form a better decision about the causal direction orientation between the nodes.

It is very important that you output the final Causal graph within the tags `<Answer></Answer>` otherwise your answer will not be processed.

Example:

Input: Nodes: [‘A’, ‘B’, ‘C’, ‘D’];

Description of Nodes: [(description of Node A), (description of Node B), (description of Node C), (description of Node D)]

Output: `<Answer>[(‘A’, ‘B’), (‘C’, ‘D’)]</Answer>`

Question:

*Input: Nodes: **{Triplet Nodes Input}***

*Description of Nodes: **{Description of Each Node from the Triplet}***

Output:

Table A24: The *triplet* query template, which includes a concise context of the graph, the input triplet nodes and their respective descriptions. As an example, for the Child graph, the context is "to model congenital heart disease in babies", the three nodes may be ('HypoxiaInO2', 'Grunting', 'GruntingReport'); and their node descriptions are ["hypoxia when breathing oxygen", "grunting in infants", "report of infant grunting"] respectively.

2106
2107
2108
2109
2110
2111
2112
2113
2114
2115
2116
2117
2118
2119
2120
2121
2122
2123
2124
2125
2126
2127
2128
2129
2130
2131
2132
2133
2134
2135
2136
2137
2138
2139
2140
2141
2142
2143
2144
2145
2146
2147
2148
2149
2150
2151
2152
2153
2154
2155
2156
2157
2158
2159

Input: (**'HypDistrib'**, **'LowerBodyO2'**)

Answer: Low oxygen areas equally distributed around the body can affect the level of oxygen in the lower body by reducing the amount of oxygen available for circulation. Therefore, the answer is $\langle \text{Answer} \rangle A \langle / \text{Answer} \rangle$.

Input: (**'Disease'**, **'LungFlow'**)

Answer: Infant methemoglobinemia is a condition where the blood is unable to carry enough oxygen, which can lead to low blood flow in the lungs. Therefore, the answer is $\langle \text{Answer} \rangle A \langle / \text{Answer} \rangle$.

Input: (**'CardiacMixing'**, **'HypDistrib'**)

Answer: Mixing of oxygenated and deoxygenated blood is a common cause of congenital heart disease in babies. This mixing can occur due to structural defects in the heart, such as a hole between the heart chambers or abnormal connections between the blood vessels. This mixing can lead to low oxygen areas equally distributed around the body. Therefore, the answer is $\langle \text{Answer} \rangle B \langle / \text{Answer} \rangle$.

Table A25: Example LLM (GPT-3.5-turbo) outputs for estimating the causal direction between a given pair of nodes (with their descriptions) using the CoT Prompt (refer Table A16 in Appendix for the prompt). Given a pair (X,Y), Option *A* refers to X causing Y, option *B* refers to Y causing X, and option *C* refers to no causal relationship between the variables. The pairs shown are from the *Child* graph from BNLearn repository (Scutari & Denis, 2014), that is used for modeling Congenital Heart Disease in infants.

Input: (**'Right C7'**, **'Discoligment injury C6-C7'**)

Answer: Discoligment injury C6-C7 can cause compression of the nerve roots that exit the spinal cord at the C7 level, which can lead to symptoms such as pain, numbness, and weakness in the right C7 dermatome. Therefore, the answer is $\langle \text{Answer} \rangle B \langle / \text{Answer} \rangle$.

Input: (**'Right C7'**, **'Left C7'**)

Answer: Right C7 and left C7 are both parts of the cervical spine and are not known to directly influence each other. Therefore, the answer is $\langle \text{Answer} \rangle C \langle / \text{Answer} \rangle$.

Input: (**'Right elbow trouble'**, **'Left shoulder trouble'**)

Answer: There is no direct causal relationship between right elbow trouble and left shoulder trouble. They may both be symptoms of a larger underlying condition, but they do not directly cause or affect each other. Therefore the answer is $\langle \text{Answer} \rangle C \langle / \text{Answer} \rangle$.

Table A26: Example LLM (GPT-3.5-turbo) reasoning outputs for estimating causal directionality between different pairs of nodes using CoT queries (refer Table A16 for the query) for Neuropathic subgraph (used for pain diagnosis).